


1-1-2014

A Principal Component Analysis of Vertical Temperature Profiles for Tracking Movements of Swordfish *Xiphias gladius*

Kathryn G. Carmody
Nova Southeastern University

Follow this and additional works at: https://nsuworks.nova.edu/occ_stueta

 Part of the [Marine Biology Commons](#), and the [Oceanography and Atmospheric Sciences and Meteorology Commons](#)

Share Feedback About This Item

NSUWorks Citation

Kathryn G. Carmody. 2014. *A Principal Component Analysis of Vertical Temperature Profiles for Tracking Movements of Swordfish Xiphias gladius*. Master's thesis. Nova Southeastern University. Retrieved from NSUWorks, Oceanographic Center. (37)
https://nsuworks.nova.edu/occ_stueta/37.

This Thesis is brought to you by the HCNSO Student Work at NSUWorks. It has been accepted for inclusion in HCNSO Student Theses and Dissertations by an authorized administrator of NSUWorks. For more information, please contact nsuworks@nova.edu.

NOVA SOUTHEASTERN UNIVERSITY OCEANOGRAPHIC CENTER

A Principal Component Analysis of Vertical Temperature Profiles for Tracking
Movements of Swordfish *Xiphias gladius*

By

Kathryn G. Carmody

Submitted to the Faculty of

Nova Southeastern University Oceanographic Center

in partial fulfillment of the requirements for

the degree of Master of Science with a specialty in:

Marine Biology

Nova Southeastern University

2014

**Thesis of
Kathryn G. Carmody**

Submitted in Partial Fulfillment of the Requirements for the Degree of

**Masters of Science:
Marine Biology**

Nova Southeastern University
Oceanographic Center

December 2014

Approved:

Thesis Committee

Major Professor : _____
David Kerstetter, Ph.D.

Committee Member : _____
Arthur Mariano, Ph.D.

Committee Member : _____
Bernhard Riegl, Ph.D.

TABLE OF CONTENTS

Table of Contents	i
Abstract	ii
Acknowledgements	iii
List of Figures	iv
List of Tables	vi
Introduction	1
<i>Swordfish Biology & Ecology</i>	1
<i>Swordfish Migration</i>	2
<i>Swordfish Management</i>	3
<i>Tagging</i>	5
<i>Light-level Geolocation</i>	8
<i>PCA Model Overview</i>	11
Materials & Methods	14
<i>Satellite Tagging</i>	14
<i>Data Analysis</i>	15
<i>Principal Component Analysis</i>	16
<i>Bilinear Algorithm</i>	16
<i>Error Metric</i>	30
Results	35
<i>Comparison Analyses</i>	35
<i>Swordfish Projection</i>	35
<i>Method Refinement</i>	59
Discussion	65
Literature Cited	69

ABSTRACT

Electronic pop-up satellite archival tag (PSAT) technology has been successfully used to monitor the at-large behavior of a suite of pelagic animals, especially regarding habitat utilization. Additionally, algorithms using ambient light-level data have allowed the derivation of geolocation estimates along the duration of the deployment. However, the diel behavior of swordfish moving below the photic zone during daylight hours precludes this methodology because of the lack of ambient light-level data. To produce deployment tracks for swordfish, a mathematical model was created to analyze hydrographic temperature and pressure data recorded by PSATs. This hydrographic-based model applies Principal Component Analysis (PCA) to vertical temperature profiles in order to estimate the movement between the initial location of release and the location of the first tag transmission. PSAT data from swordfish (n=4), blue marlin (n=13), white marlin (n=2), and black marlin (n=1) were used to generate daily coordinate estimates. The marlin data provided sufficient light information to derive geolocation estimates using two light-based state space models, while the hydrographic PCA model was used to derive comparison estimates. Comparisons of the two models show an average root mean square error of 174.3 km with a standard deviation of 119 km. These results demonstrate the ability of this PCA model to extract the movement of tagged fish with consistent reasonable accuracy, within 1-2 degrees of light-based estimations. This study shows the feasibility of using temperature and depth data instead of light levels to allow effective tracking of swordfish and any species that demonstrate crepuscular diving behavior.

ACKNOWLEDGEMENTS

I would like to thank my major advisor, Dr. David Kerstetter, Nova Southeastern University, for his assistance and dedication to this thesis project. I would like to thank my committee member Dr. Arthur Mariano, University of Miami, for his statistical guidance and support throughout this study. I thank committee member, Dr. Bernhard Riegl, Nova Southeastern University, for assistance with the methods carried out in R. I would like to thank Clarence Flowers (Orchid Development, LTD) for his investment in the NSU Fisheries Laboratory's ongoing swordfish research in the Cayman Islands, as well as the invitation to take part in the Cayman Swordfish Challenge Tournament for two consecutive years. I thank Captain Bouncer Smith and the entire crew of *Arcturus*, who dedicated their fishing time and swordfish for tag and release both years. I would like to thank my labmates, Travis Moore, Jenny Fenton, and Jesse Secord for their efforts in the field. A special thank you to John E. Graves (Virginia Institute of Marine Science) and the International Game and Fishing Association in collaboration with Stanford University for sharing their data from PSAT deployments, without which this study could not have been possible. I would also like to thank my family and friends for their continued support throughout the duration of this study.

LIST OF FIGURES

Figure 1. The reconstruction of a temperature profile using temperature and depth data from a Microwave Telemetry, Inc. model PTT-100 tag deployed on swordfish #61665 in the Caribbean Sea. From left to right, (a) raw profile using all temperature and depth records received by the tag during the first day of deployment; (b) the raw profile is interpolated and averaged at every 20 m depth to a max depth of 600 m.

Figures 2. Daily temperature profiles recreated using Microwave Telemetry, Inc. model PTT-100 tags deployed on blue marlin (n=7) interpolated and averaged at every 5 m depth.

Figures 3. Temperature profiles recreated using data from Wildlife Computers, Inc. model Mk10 PATs deployed on blue, white, and black marlin (n=9). The temperature and depth data from each day is interpolated and averaged every 5 m depth. On the left is the profile of the initial deployment coordinates, and on the right is the profile of the final day used for our analysis.

Figures 4. Estimates of marlin tagged with Microwave Telemetry, Inc. model PTT-100 tags (n=7) as given by the hydrographic PCA model and the light-based model, *TrackIt*. The locations of fish release and final tag pop off are highlighted.

Figures 5. Fish tracks of marlin tagged with Wildlife Computers, Inc. model Mk10 PATs (n=9). On the left is the track derived from the hydrographic PCA model, while on the right are the estimates from a light-based state-space model that uses the tag's raw global positioning estimates and incorporates satellite sea-surface temperature (SST).

Figures 6. Root mean square error (RMSE) comparisons plotted over time for three track derivation models from electronic tag data. RMSE is calculated by comparing each latitude and longitude estimate produced by the introduced hydrographic PCA model and

two different light based models. Light data from Microwave Telemetry, Inc. model PTT-100s were run through the light-based model *TrackIt* to produce geolocation estimates (Figures *a-c*). Wildlife Computers, Inc. model PATs generate raw global positioning estimates that were put into a state-space model that incorporates satellite sea-surface temperature (SST) to derive the most accurate light-based locations (Figures *d-f*).

Figure 7. Root mean square (RMSE) plotted according to the length of tag deployment. Days-at-large (DAL) ranged from 9 to 120 days. A correlation can be seen in the longer tag deployments yielding larger error calculations.

Figures 8. Temperature profile recreated for the initial and last coordinates of swordfish tagged with Microwave Telemetry, Inc. model PTT-100 tags (n=4). The temperature and depth data was interpolated and averaged at every 20 m depth each day.

Figures 9. Fish tracks of swordfish tagged with Microwave Telemetry, Inc. model PTT-100 tags (n=4) created from the hydrographic PCA model. The locations of fish release and final tag pop off are highlighted. The top image is a latitude and longitude plot with each estimate labeled numerically by day. The bottom image is a Google Earth map of the general track and the directions taken by the fish according to our analysis.

Figure 10. Fish tracks of blue marlin (n=3) tagged with Microwave Telemetry Inc. PTT-100 tags (n=3) as given by the PCA model analysis and residual calculations. These refined estimations are calculated by subtracting the residual values and allow for non-linear movement to be demonstrated.

LIST OF TABLES

Table 1: Summary of the tag deployments and reporting data, including species, tag PTT identification number, tag model, geographic region of tag deployment (VZ = Venezuela, VI = Virgin Islands, NC = North Carolina, ZA = South Africa, POR = Portugal, MR = Morocco, US = United States, CZ = Cayman Islands), days-at-large, date of release, date of first ARGOS transmission, and net displacement (km).

Table 2: Summary of comparison analyses by species, including species, tag PTT identification number, tag model, and root mean square error (RMSE) averaged over the tagging duration (km), maximum depth recorded by the tag (m), and average depth recorded by the tag (m).

Table 3: Error (km) of hydrographic PCA model as compared to two light-based models using data received from two types of tag models (MWT = Microwave Telemetry, WC = Wildlife Computers). Light data from Microwave Telemetry PTT-100s (n=7) were run through light-based model *TrackIt*. Global positioning estimates of Wildlife Computer Mk10 PATs (n=9) were run through a state-space model incorporating satellite SST. Error is given by calculating the root mean square error of both latitude and longitude estimates, and averaging the values over the course of the tag duration.

Table 4: Error of PCA model variations used to determine the optimal number of principal components to use in our analyses. Species code, tag ID number, average error (RMSE values) given by our PCA model analysis of PTT-100 (Microwave Telemetry, Inc.) data (n=7) incorporating the first computed principal component (PC) only, both the first and second PC, and the first PC residual calculations. Average RMSE values are in kilometers. The variances described by the respective PCs are given as a percentage.

INTRODUCTION

Swordfish Biology and Ecology

Swordfish *Xiphias gladius* Linnaeus, 1758 is a monogeneric species that diverged from the Istiophorids (billfishes) approximately 3 million years ago (Dewar et al 2011, Fierstein and Stringer 2007). Swordfish can be phenotypically differentiated by their bill - flat in cross-section - and lack of denticles. The life history of swordfish has been completely described by Govoni (2003). Young swordfish exhibit rapid growth reaching about 130 cm measuring lower jaw-fork length (LJFL) by Age two (NMFS 2008). Swordfish are characterized by dimorphic growth. Females reach maturity by Age five at an average length of 180 cm LJFL, while males reach maturity at one to two years of age at about 129 cm LJFL (Taylor and Murphy 1992, Arocha 2003, NMFS 2006). Swordfish are multiple spawners and capable of spawning throughout the year. The spawning dates and abundance of larvae for North Atlantic swordfish strongly suggest that the southeastern Caribbean Sea, Gulf of Mexico, and waters inshore of the Gulf Stream in the Florida Straits all serve as nurseries (Arocha 2003, Govoni 2003).

Swordfish are distributed worldwide among tropical, semi-tropical and temperate waters between 45° N and 45° S (Palko et al. 1981, Sedberry and Loefer 2001, Loefer et al. 2007). They are an oceanic species, but can be found in coastal waters above the thermocline. Large-scale movements are commonly associated with oceanographically distinct regions. Previous tagging studies have revealed seasonal movements over 2,000 km in length (Sedberry and Loefer 2001, NMFS 2008). These extensive migrations are likely driven by spawning and feeding behaviors (Young et al. 2006).

The swordfish is a pelagic apex predator found to inhabit regions of high food availability (Palko et al 1981, Abascal et al. 2015). Fine-scale movement studies (Sepulveda et al. 2010, Dewar et al 2011) support a typical foraging strategy strongly associated with movement of the deep sound scattering layer (DSL). The DSL is associated with the vertical distribution of crustaceans and gelatinous zooplankton. Also referred to as the “false bottom,” this dense accumulation of organisms is primarily driven by predator avoidance (Frank and Widder 2002). Studies on the feeding ecology

of swordfish support a diet consistent with mesopelagic fishes, such as bigeye tuna *Thunnus obesus*, that exhibit vertical migrations. Stomach content have included mostly cephalopods and a variety of nektonic and micronektonic fishes (Carey and Robinson 1981, Heemsoth 2010). There is evidence of an ontogenic diet shift resulting in the consumption of larger cephalopod prey as swordfish grow (Young et al. 2006).

Variability in catch rates support undetermined factors that influence swordfish movement and aggregations. This includes locations of oxygen minimum zones (OMZ), thermal boundaries, and ocean mixed layer (OML) depths, seabed topography, and chlorophyll concentrations (Sepulveda et al. 2010, Luckhurst 2007, Young et al. 2006, Carey and Robinson 1981). Reports of behavioral changes in relation to the lunar cycle are also evident; a positive correlation exists between the maximum depth reached by the swordfish and lunar illumination (Dewar et al. 2011, Lerner et al. 2013, Abascal et al. 2015). Following isolume depths would allow swordfish maximum visual acuity for hunting success (Carey and Robinson 1981, Loefer et al. 2007). This is consistent with known foraging behavior, as the depth of the deep scattering layer (DSL) is also deeper when light penetrates farther down (Dewar et al. 2011).

Swordfish Migrations

The migration of swordfish is one of the most complex among pelagic fishes (Palko et al. 1981). Previous swordfish tagging studies in the Atlantic, Pacific, and Mediterranean Sea have revealed movement and distribution patterns that vary considerably with season, gender, and ocean basin (Sedberry and Loefer 2001, Neilson and Smith 2010, Sepulveda et al. 2010, Dewar et al. 2011). Acoustic tracking studies, fisheries data, and pop-off satellite archival transmitters have determined two generalized movements exhibited by swordfish in the North Atlantic (Fenton 2012). Swordfish exhibit strong latitudinal movement, migrating northeast in the early summer and southwest during the autumn (Palko et al. 1981, NMFS 2006). Neilson et al (2009) showed that swordfish tagged in Canadian waters exhibited a consistent, long distance migration pattern (Abascal et al. 2015, Neilson et al. 2009). Specifically, swordfish were seen occupying temperate waters north of 40° N latitude early June through October, then by early January swordfish were in the warm waters of the Caribbean where they reside

until April before resuming their northward migration (Neilson et al. 2009). Another movement trend common to swordfish in the North Atlantic is a migration west toward the continental shelf during the summer and east into deeper waters during the autumn (Palko et al 1981).

A generalized vertical movement pattern has been well defined by archival tagging studies (Loefer et al. 2006, Neilson et al. 2009, Sepulveda et al. 2010, Dewar et al. 2011, Fenton 2012, Lerner et al. 2013). Swordfish demonstrate strong diurnal trends where daylight hours are spent at depths of 300-1000 m and night hours are spent at near-surface waters, with night depths also varying slightly by moon phase (Carey and Robinson 1981, Sepulveda et al. 2010, Lerner et al. 2013). The “U”-shaped diving pattern driven by resource availability is consistent with swordfish in all ocean basins (Loefer et al. 2006, Sepulveda et al. 2010, Dewar et al. 2011, Lerner et al. 2013). This diel vertical movement has been well documented for swordfish and other large predators associated with foraging in the DSL (Dewar et al. 2011). The only deviation from this trend is known as a basking event, in which a swordfish rests at the surface during the daytime (Sepulveda et al. 2010), anecdotally believed to increase digestion rate in warmer surface waters. Previous tagging studies have characterized this basking behavior by a rapid ascent during the day, prolonged surface interval, followed by a rapid return to depth (Dewar et al. 2011). Although basking events have been observed in both warm tropical and cool temperate waters, they are more prevalent in cooler regions (Dewar et al. 2011). A correlation between the size of the swordfish and periodicity of these events likely supports this behavior as a way to increase metabolic rates after foraging in cooler waters (Sepulveda et al. 2010). The variability of horizontal movements and vertical behavior highlights the need for additional information on swordfish habitat utilization and fine-scale movements.

Swordfish Management

Swordfish is defined as a highly migratory species (HMS) by the Magnuson-Stevens Conservation and Management Act (MSFCMA). Commercial fisheries target swordfish extensively throughout its latitudinal range using pelagic longline gear (PLL), drift gillnets (DGN), and to a lesser extent harpoon fishing gear (Sepulveda et al. 2010,

Luckhurst 2007). The commercially valuable flesh has helped make swordfish a global commodity (Loefer et al. 2007). The rapid development of swordfish fisheries has led to a steady increase in global swordfish landings since the 1980s (Sepulveda et al. 2010). Unfortunately, much uncertainty remains regarding the status of swordfish stocks. A main limitation to current stock assessments is the lack of knowledge in stock structure and population boundaries (Abascal et al. 2014).

Internationally, Atlantic swordfish fall under the authority of the International Commission for the Conservation of Atlantic Tunas (ICCAT) based in Madrid, Spain. ICCAT recognizes two stocks in the Atlantic, dividing the population into north and south stocks at 5°N latitude (there is also a small population in the Mediterranean Sea that is managed separately). Under the authority of the Atlantic Tuna Convention Act (ATCA) of 1975, the United States is required to abide by national standards set by ICCAT based on annual Standing Committee on Research and Statistics (SCRS) stock reports. According to the Magnuson Act of 1990, U.S. domestic fisheries management falls under the responsibility of the Secretary of Commerce via the various Regional Fisheries Management Councils. The amended Magnuson Act (Magnuson-Stevens Act) of 1999, however, elevated the authority of all HMS governance from the Councils directly to the Secretary of Commerce, which manages HMS species through the National Marine Fisheries Service (NMFS 1999).

During the 1980s and 1990s, the North Atlantic swordfish stock experienced reduced catch rates and smaller average fish size (SCRS 2009). Concern for the sustainability of the fishery at present exploitation rates led ICCAT to establish a ten-year rebuilding plan in 1999. This plan reduced the annual total allowable catch (TAC) to 14,000 metric tons, and included country-specific allocations, increasing the U.S. quota to 30.49 percent of the TAC (SCRS 2009). In an attempt to protect juveniles before they have had a chance to spawn, NMFS instituted a series of time-area closures for PLL vessels in the Gulf of Mexico and along the southeast Atlantic coast. A cooperative effort led by sustainable fishing gear and public support, such as the “Give Swordfish a Break” campaign, has helped rebuild the North Atlantic stock and consequently re-establish the U.S. recreational swordfish fishery.

More recently, concern has been raised over the interaction of swordfish fisheries with non-target species. In attempts to reduce the incidental takes of protected species, additional management restrictions have been implemented. These bycatch reduction strategies include bycatch quotas and encouraging the use of alternative gear types, such as swordfish buoy gear (Sepulveda et al. 2010, NMFS 2006). Buoy gear was authorized for the U.S. Atlantic waters in 2006 as a permissible gear type for commercial swordfish fisheries (NMFS 2006). Catch reports show the use of buoy gear increases selectivity (CPUE) and reduces bycatch interaction (SRCS 2009).

The North Atlantic swordfish stock has experienced growth in recent years, due to ongoing U.S. domestic and international measures aimed at reducing mortality, protecting juveniles, reducing bycatch, monitoring international trade, and improving data collection (NMFS 2010). According to stock reports by ICCAT, the swordfish population was rebuilt merely seven years following the rebuilding plan implementation (NMFS 2010). By the end of the ten-year deadline in 2009, there was greater than 50 percent probability that the stock was at or above the biomass needed to achieve maximum sustainable yield (MSY), and thus the population was then considered successfully rebuilt (SCRS 2009). The most recent stock assessments have shown the North Atlantic stock to be five percent above the target level (SCRS 2009, NMFS 2010). Despite apparent management success, much uncertainty remains in the Atlantic-wide swordfish stock assessments. This can be attributed to the continuing need for additional knowledge regarding the migration routes, movement, and distribution patterns of swordfish within and between the managed stocks.

Tagging

Traditional tagging, using conventional (non-electronic) tags that are dependent on recapture, has proven useful in determining long-term movement and growth (Sedberry and Loefer 2001). The high commercial importance of swordfish has helped fuel a large conventional tagging effort since the 1950s, mainly through the NOAA Cooperative Tagging Center based in Miami, FL. These tags have provided much needed information on swordfish growth as well as large-scale movement trends

(Luckhurst 2007). However, low recapture rates and tag recovery (approximately 3.6% for swordfish, per ICCAT 2009) have limited these fishery-dependent efforts.

Electronic tracking devices are made up of two tagging systems - telemetry and archival devices. Developed in the 1950s, acoustic telemetry tags are the first electronic tags to be widely used in ocean studies. Acoustic telemetry tags work with hydrophone array or active sonar. These systems detect an ultrasonic, high frequency “ping” delivered from the tag when in appropriate range. Hydrophones are typically mounted to vessels, or deployed on automatic recorders moored in a specific region. Acoustic telemetry tags have been successfully used to determine movement on a small spatial scale, and have helped determine locations of fish aggregation, and spawning (Sibert and Nielsen 2001).

Satellite telemetry tags work with Argos satellite system to determine global positions. Tags integrated with an Argos-certified transmitter, or ‘platform,’ can send signals to the Argos satellite when within range. Signals are received on average, every 10 minutes where they are stored and retransmitted to a ground database every time the satellite passes over a receiving station. The Argos network requires three or more transmissions from the tag in order to obtain positioning (Argos 2014). Radio waves received by satellites cannot pass through water, so transmissions are not received if the tag is submerged. Therefore satellite telemetry only works well with terrestrial animals or marine organisms that surface for prolonged periods of time (e.g. cetaceans). Standard Global Positioning System (GPS) technology is similarly unsuitable for pelagic fish as it requires up to a few minutes of tag exposure in order to determine locations (Evans et al. 2011).

Electronic archival tags, first deployed in the 1990s, are clock-integrated data storage devices equipped with multiple sensors (Sibert and Nielsen 2001). Archival tags allow data to be electronically stored until fish recapture and tag recovery (Arnold and Dewar 2001). The tags can be surgically implanted or attached to the exterior of the fish via an anchoring device (Musyl et al. 2003). These electronic devices record ambient variables at specified sampling frequencies. Equipped with sensors, including temperature, pressure, and light, archival tags have provided high quality data over long periods of time. The sampling of fish environment has contributed immensely to our

understanding of migrations, habitat utility, and behavior (Fenton 2012). Archival tagging studies in the North Atlantic (Carey and Robinson 1981, Sedberry and Loefer 2001, Lerner et al. 2013), West Pacific, and Eastern North Pacific (Carey and Robison, 1981) have worked to categorize the strong diurnal behaviors typically exhibited by swordfish.

Pop-up satellite archival tags (PSAT) are integrated with the combined technology of satellite telemetry and archival data storage tags. The development of PSAT technology has allowed researchers to obtain data stored without tag retrieval, and in doing so, drastically improved the rate of data recovery. “Pop-up” tags were introduced in the late 1990s to track large pelagic fishes (Arnold and Dewar 2001, Fenton 2012). PSATs are equipped with three sensors that record ambient variables including temperature, pressure (converted to depth), and light intensity at specified sampling frequencies. These electronic devices are programmed to release from the animal at a preset date. Once the tag reaches the sea surface following release from the animal, the stored data is automatically transmitted to an Argos satellite. To prevent destruction of the tag and loss of data, PSATs are programmed with mechanical and electronic (programmed) ‘fail-safe’ releases (Nielsen et al. 2006). These premature releases allow for early data transmission in case of tag attachment failure. A pressure release mechanism is triggered when the tag nears a depth at which it will be crushed. Premature release programming activates when the tag experience little pressure change for a prolonged amount of time (Musyl et al. 2003, Sibert and Nielsen 2001, Nielsen et al. 2006, Fenton 2012).

Since their introduction in 1997, PSATs have revealed large-scale movements of large pelagic fish, as well as behavioral patterns and fine-scale, diel movements. The use of PSATs allow researchers to overcome many of the limitations provided by acoustic and conventional tagging (Fenton 2012), and they are considered “fishery independent,” as they do not need to be returned by a fishery recapture to attain the data they collect (Musyl et al. 2003). The data retrieved has been critical to understanding the physical and physiological variables that relate fish behavior to its surrounding environment (Arnold and Dewar 2001). These data typically include habitat preferences, seasonal movements, and potential mixing of stocks. A three-year research program using PSATs

by Neilson and Smith (2010) supported North and South movement between Grand Banks and the Caribbean, but little movement from the NW Atlantic to the NE Atlantic. This suggests the potential for two separate swordfish populations in the North Atlantic. The same study also demonstrated a possible homing behavior as the swordfish were seen returning to Georges Bank consistently each year to feed (Neilson and Smith 2010). Trends in spawning and feeding behavior as well as residence sites, and oceanic migrations are all needed to manage this resource (Ortiz 2003). In contrast with vertical movements and behavior patterns, there has been limited information collected on swordfish horizontal movement or how individuals are influenced by local environment conditions.

During the early years of development, electronic devices experienced various failures that complicated their usage. Their limited use stemmed from the relatively high costs, low tag retention, high fish mortality, transmitter recovery, variable reporting rates, and amount of transmitted data (Nielsen et al. 2006). Such limitations have been addressed in recent years, and have led to the smaller, high capacity tags equipped with multiple ‘fail safe’ mechanisms used today

Light-level Geolocation

As the archival tag technology improves, their use has become an indispensable tool for fishery biologists. Since satellite telemetry via Argos or GPS is unavailable underwater, alternative methods must be used to locate tags deployed on marine organisms. These geolocation methods are complex and not always as effective as needed. The systematic and random errors associated with geolocation have limited the use of tagging technology (Nielsen and Sibert 2007, Musyl et al. 2003). Despite frequent improvements, researchers continue to demand higher levels of accuracy in geolocation estimates by light records (Sibert and Nielsen 2001).

The use of light data to geographically position the tag has been the primary method for locating satellite tags (Lam et al. 2010). Light-based geolocation uses recorded light levels and time of day to estimate the position of the sun and consequently determine the global position. Longitude is calculated via a determination of local noon, when the angle between the sun and vertical (zenith angle) is zero (Hill and Braun 2001).

Latitude is computed from the length of time between sunrise and sunset, or when the zenith angle is 90 (Hill and Braun 2001, Nielsen and Sibert 2007).

For marine animals that demonstrate near- or at-surface behaviors, these methods are generally reliable (Nielsen and Sibert 2007). However, the diving behaviors typical of deep-diving marine animals significantly degrade the accuracy of these light-based geolocation methods through increased light attenuation at depth (reviewed by Teo et al. 2004). The accuracy of light-based geolocation estimates can also be affected by water turbidity, weather, and even the sensitivity of the PSAT light sensors used by the tag manufacturer (Hill and Braun 2001). Furthermore, due to differences between the hemispheres, latitude is subject to large error depending on the time of year. Specifically, global position estimates based on day length become increasingly inaccurate approaching the equinox, when the day length becomes the same at all latitudes for a given hemisphere (Hill and Braun 2001, Neilson and Smith 2010).

Previous studies demonstrating light-based geolocation estimates within 0.5–1 degree, used data from tags deployed on mooring buoys, ships, or fish restricted to shallow waters (Gunn et al. 1994). Thus, diving activity was not accounted for (Teo et al. 2004). Highly migratory species (HMS) that demonstrate crepuscular diving behavior exhibit diel movements that closely correlate with the DSL. These fishes, including swordfish and bigeye tuna, spend the majority of the day at depths where light does not penetrate or near the threshold of the tag's sensitivity to light. Furthermore, light levels are hardest to measure during these periods around sunrise and sunset when diving occurs (Neilson and Smith 2010).

Due to these collective factors, the raw unfiltered and uncorrected geolocation estimates derived from light records are typically very noisy, placing the tagged fish hundreds of kilometers from their actual position (Neilson et al. 2006). To overcome these inaccuracies, various mathematical methods have been coupled with the limited light-level data available to produce a relatively more accurate track.

Hill and Braun (2001) developed astronomical equations to calculate estimated times of sunrise and sunset using the limited light data. Their study introduced what is known as a threshold model in which the brightest light is referenced to establish two threshold values. A maximum threshold is set to represent when the sun is directly

overhead (noon), while a minimum threshold represents when the sun passes below the horizon (sunset). The time of sunset and sunrise can then be determined by when the light passes these thresholds each day. Latitude estimations are particularly vulnerable to this method. If thresholds set incorrectly (e.g., from cloudy conditions), the error in latitude is amplified (Lam et al. 2010, Hill and Braun 2001). Their results showed the expected variability in latitude would never be less than 0.7 degrees, equivalent to 48 nautical miles (88.9 km), no matter how effective the geolocation analysis (Hill and Braun 2001).

An alternative method for geolocation known as the template-fit model was developed by Ekstrom (2002). This method derives times of solar events based on light records and error measurements. A template based on Ekstrom's simplified geophysical model (fully described in Ekstrom 2002) takes into account how light reaches Earth's surface through the atmosphere. This template is fit to the light data, effectively matching the slopes of light curves, as sunrise or sunset approaches. The template is then adjusted according to error estimates, which include the effects of weather, latitude, and season (Ekstrom 2006).

State-space models have been used to analyze location observations over time, including complex movement patterns (Jonsen et al. 2003). A state-space model is a coupled model, consisting of a measurement and transition analysis. The measurement model describes the state of a system and observations at that time, including the light-based location and error estimations given by the threshold or template-fit models. The transition model describes the process that cannot be directly observed, or the movement from one location to the next (Sibert 2003). A state-space model creates a resulting track with error estimations that are used to create a confidence region around the track. This approach of complex modeling has allowed researchers to gather information on animal interactions with their environment.

The most recent models have incorporated a mathematical technique known as the Kalman filter (Harvey, 1990). This algorithm uses a series of noisy measurements observed over time, a dynamical model, and prior information on the error characteristics of both the data and the model to produce an estimate of unknown variables that tend to be more precise than those based on a single measurement (Hill and Braun 2001). Kalman filter state-space models are the most accurate mathematical estimators to date

for fish tracking. This model computes the position of the fish as a weighted average of two position estimates: the geolocation estimate and the one computed from the transition equation (Sibert et al. 2003, Lam et al. 2008). Sibert and Fournier (2001) developed a state-space model based on the Kalman filter, which was initially used to determine optimal estimates of satellite tagged bigeye tuna. Data were analyzed from tags deployed on bigeye tuna and compared to those attached to stationary moorings; the comparison analyses showed improved geolocation estimates. Standard deviation estimates ranged from 0.5 to 4.4 degrees latitude and 0.2 to 1.6 degrees longitude while demonstrating realistic *in situ* geolocation errors and movement parameters (Sibert and Fournier 2001, Sibert et al. 2003).

State-space models have expanded to include supplementary data, such as coastline, bathymetry, and sea surface temperatures to constrain the model (Musyl et al. 2003, Teo et al. 2004, Wilson et al. 2004, Nielsen and Sibert 2007, Lam et al. 2010). In particular, the incorporation of satellite-derived sea surface temperature (SST) data has further refined light-based geolocation estimations. By integrating SST into their Kalman filter state space model, Lam et al. (2010) found the added data improved the overall accuracy of geolocation estimates while reducing confidence regions. This has been further supported by multiple other studies incorporating SST, which similarly show a reduction in the error of light-based latitude estimates (Teo et al. 2004, Lam et al. 2010). However, these models are only significantly improved when the sampled SST is from areas of a strong thermal gradient (Nielsen et al. 2006, Fenton 2012).

The state-space model *TrackIt*, developed by Nielsen and Sibert (2007), is the first model to produce geolocation estimates based directly on light measurements recorded by the tag. Unlike the two-step approaches that utilize threshold algorithms, this model uses raw light measurements as input for the Kalman filter. Threshold models process each light measurement independently, leading to inaccuracies prior to being used for geolocation in the state-space model. *TrackIt* uses a one-step method that allows the relation between all variables, including light measurements and solar altitudes, to be estimated within the model in order to produce a most probable track (Nielsen and Sibert 2007).

PCA Model Overview

The present tracking methods discussed in the previous section are unable to incorporate all of the temperature data collected by the PSAT. A new tracking method is proposed that is based on a principal component analysis of the observed average daily temperature profiles. Principal component analysis (PCA) is a statistical method that allows for datasets to be represented efficiently by describing only the most important patterns (modes) of variability. PCA reduces the number of variables in a dataset to a smaller number of “components” that account for most of the data variance. As a statistical tool, PCA (and its various extensions) is particularly useful for analyses of large data sets, such as archival tag records, as it greatly reduces data volume and noise in the process. There are multiple variations and extensions of PCA depending on the type of data input. An eigenanalysis of the covariance matrix calculated from daily smoothed temperature profiles is performed here. The eigenvectors also known as the empirical orthogonal function are the dominant modes of vertical temperature variability. The principal components for each daily temperature profile are calculated and used to generate daily estimates of the fish position by a simple algorithm discussed below.

Temperature versus depth profiles vary over geographical area and time due to ocean dynamics and variations in ocean forcing. As the tagged fish make their diel migrations, they sample the vertical distribution of temperature over the water column (Figure 1). As the tagged fish samples different water masses, for example, by going across a front, the temperature profiles will significantly change. Thus variations in daily temperature profiles can be used to track the movement of a fish if some information about the distribution of temperature profiles with latitude and longitude is known.

PCA orders the dominant statistical modes, the EOFs by the amount of variance described by each mode, so that the first mode will describe the most variance in the variation of temperature with depth. The second EOF will describe the second largest amount of variability, and so on. The corresponding principal components (PCs) modulate each EOF by an amplitude and polarity for each of the daily temperature profiles. Polarity is set such that positive PCs imply warmer profiles and negative PCs imply cooler profiles. The PCs summarize the vertical temperature profile variability.

PCs combined with information or a model on how temperature profiles vary with longitude and latitude is used here to calculate fish tracks.

An algorithm was written to derive position via a bilinear analysis of the calculated PCs and known coordinates of the tag deployment and pop-up locations. The algorithm assumes and calculates a linear spatial function between the PCS for both the longitude and latitude of the deployment and pop-up positions for each fish tag deployment. All of the daily PCs and the linear function for longitude and latitude are used to generate a set of daily coordinates of the fish positions. The set of daily coordinates from the algorithm are used to generate the horizontal fish track for the deployment period. The objective of this study is to introduce a statistical model using hydrographic data to derive geolocation estimates of satellite tagged fish comparable to current light-based models.

MATERIALS & METHODS

Satellite Tagging

Four Microwave Telemetry high rate (HR) PTT-100 tags were deployed on swordfish caught and released at night during the annual Cayman Swordfish Challenge fishing tournament held during the spring of 2012, 2013, and 2014. Tagging was performed using methods described in Fenton (2012). Data from PSATs deployed on marlin in 2008, 2009, 2011, 2012 and 2013 were reanalyzed in the comparison portion of this study. Microwave Telemetry (MWT) PTT-100 HR tags were rigged and deployed on blue marlin in the Caribbean as described in Graves and Horodysky (2005).

Platform Transmitter Terminals (PTTs) send signals to satellites once the antennae breaks the surface at pop off. The data is relayed to ground stations where it is electronically transferred to processing centers to be made available to researchers. These PTTs are 166mm by 41 mm anchored with a 171mm antenna, and weighing 65 to 68 grams. This small size and weight prevents major drag and potential alteration in swimming behavior when attached to large teleosts. (Graves and Horodysky 2010, Fenton 2012). The tags were programmed to record measurements every 90-120 seconds. The temperature sensor ranges from -4 to 40 C with a resolution of 0.16 to 0.23C. Rated to 3000 psi, depth is recorded 0 to 1296 m with a resolution of 5.4 m.

Unfortunately, the high sampling rate programming, including the increased depth resolution, results in decreased resolution in light level data due to on-board data storage limitations. The light sensitivity of these tags is therefore less than 4×10^{-5} lux (1 lumen) at 555 nm and does not allow for raw geolocation estimates to be generated by the tag itself. To generate estimates, the light data received was run through a light-based model. These tags can be programmed to release for up to thirty days following activation. PTT-100 HR tag deployments for this study ranged from 9 to 29 days.

Mk10 and Mini-PAT popup archival tags (PATs) manufactured by Wildlife Computers (Redmond, Washington, USA) were deployed on blue marlin *Makaira nigricans*, black marlin *Istiompax indica*, and white marlin *Kajikia albida* (formerly *Tetrapturus albidus*) as part of the International Game and Fishing Association (IGFA)

International Great Marlin Race (IGMR). Both tags models are pressure rated to 2000 m, and are equipped with sensors to record and store temperature, depth, and light data. The Mk10 has a memory capacity of 1 gigabyte, while the MiniPAT restricted by its smaller size, stores up to 16 megabytes of memory. The temperature sensors have a resolution of 0.05°C with a range of -40° to 60°C and -5° to 45°C for the Mk10 and MiniPAT respectively. The depth sensor of both tag models is rated to 1700 m with 0.5 m resolution. Light sensitivity ranges from $5 \times 10^{-12} \text{ W cm}^{-2}$ to $5 \times 10^{-2} \text{ W cm}^{-2}$. The MiniPAT also includes two light sensors to reduce noise, each measuring at an optimum 440 nm wavelength.

Both PAT models are optimized for post-deployment geolocation estimation. Wildlife Computers offers software (Wildlife Computers Global Position Estimator Version 2) that processes the high-resolution light records to produce global positioning estimates (GPEs). A light-based algorithm uses the light data collected by the tag with dawn and dusk light curves to generate the GPEs (Wildlife Computers 2014). The maximum length of deployment for both Wildlife Computers tag models is two years. The Mk10 and MiniPAT data used for this study came from deployments ranging from 28 to 180 days.

Data Analysis

Archived data are relayed in hexadecimal code by the floating PSAT through the ARGOS satellite system. Once the PTT-100 HR completed its transmission, data reports containing time-series depth, and time-series temperature are decoded, compiled into Excel files, and sent to the researcher via email (Microwave Telemetry 2013). For our analyses, the archived depth and temperature data are imported from .csv files into R, where the daily temperature profiles are extracted. Interpolation of these profiles is performed by averaging the temperature at each 5 m (marlin) or 20 m depth (swordfish data) interval for each day. Maximum depth was determined by looking over all individual tag data records and ranged from 80m to 200m for marlin and 460-600m for swordfish.

Temperature and depth data from WC PAT tags are presented in histograms. Unlike the Microwave Telemetry PTTs, raw temperature and depth records are not given

in the processed files. Rather, the archived temperature and depth data are compressed into data bins set at pre-determined sampling intervals. Time-at-temperature (TAT) and time-at-depth (TAD) summary histograms are presented in the data files. The histograms include depth and temperature measurements and the time at which they were sampled. PAT-style depth-temperature profiles (PDTs) are given that consists of all temperature and depth data records for that day divided into eight bins of equal size. For each bin depth, a minimum, maximum, and mean temperature is given (Wildlife Computers 2014). In order to create a more specific temperature profile attributed to each day, these eight data points were interpolated in our analyses to generate measurements, on average, every 5 m depth.

Principal Component Analysis

Temperature profiles were constructed by fitting cubic splines to each set of daily temperature measurements (Fig. 1), and then evaluating the splines at fixed vertical depths that depended on the fish species (Figures 2, 3). An average profile was calculated by averaging all of the daily profiles, and it was used to de-trend each daily profile for the covariance calculation. The covariance matrix is between residual temperature at different depths and is calculated by averaging over all of the profiles. The PCs are calculated by regressing the residual temperature profiles onto the EOFs. Based on preliminary calculations, the second EOF and its PCs explained an insignificant amount of variability so that their distribution did not aid in tracking the fish. For the data analyzed here, the first mode explains 85-95% of the variance, while the second mode only explains 2-10% of the variance.

Bilinear algorithm

An algorithm incorporates the PCs and the initial and final positions from the coordinates of tag deployment and first transmission. This equation calculates the estimated coordinates for each respective day during the tag deployment. The vectors of known longitude and latitude are given by:

$$\begin{bmatrix} X_1 \\ X_n \end{bmatrix} \quad \begin{bmatrix} Y_1 \\ Y_n \end{bmatrix}$$

Figure 1.

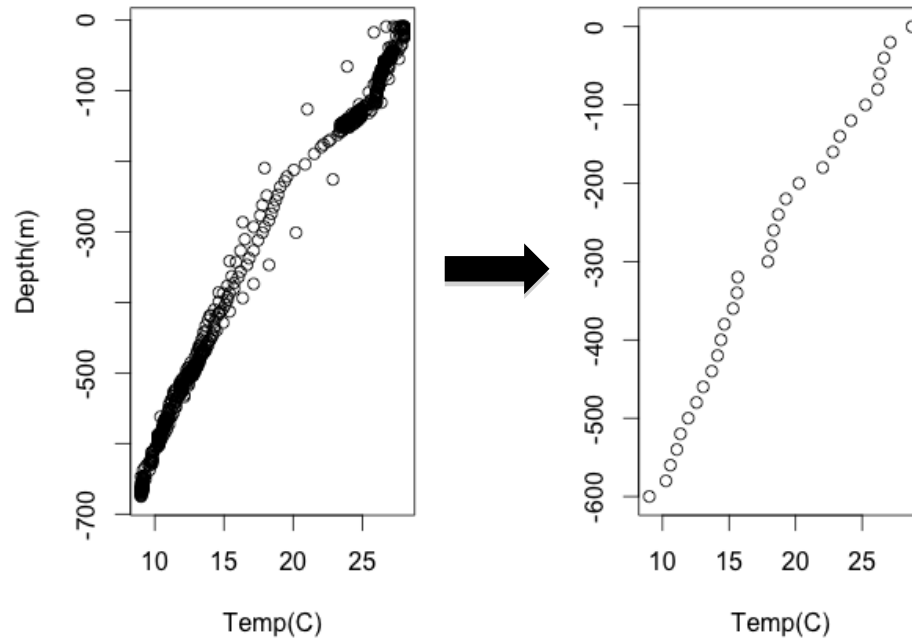
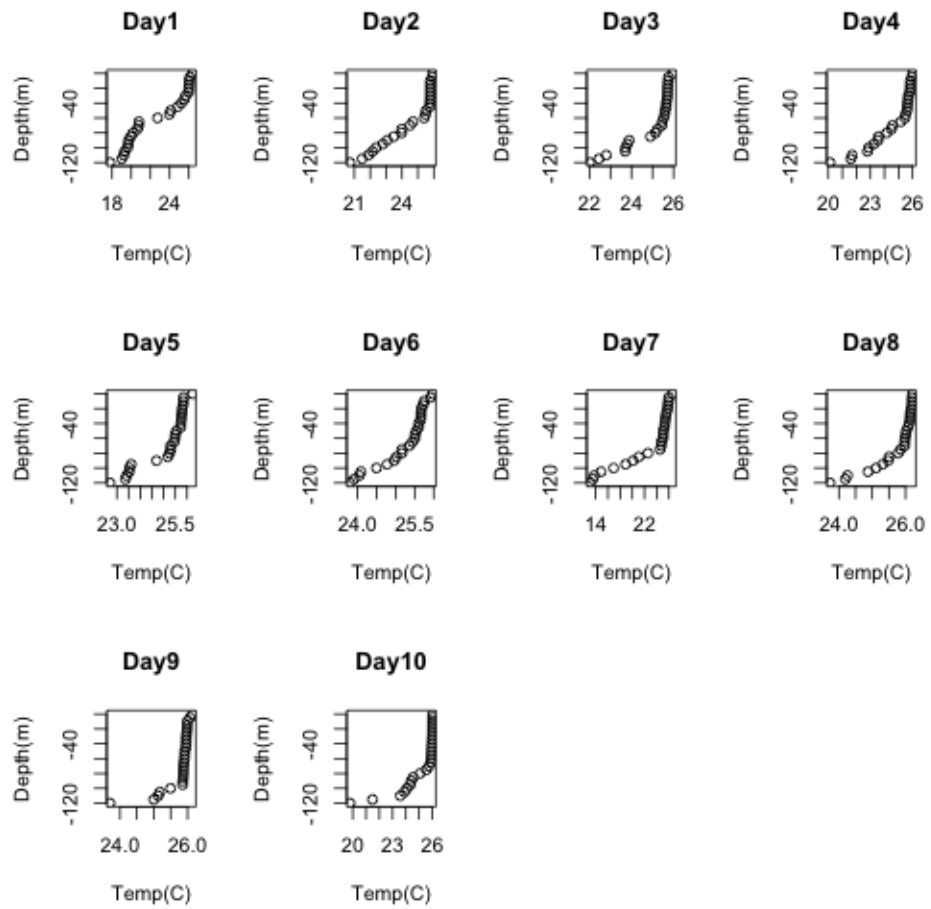
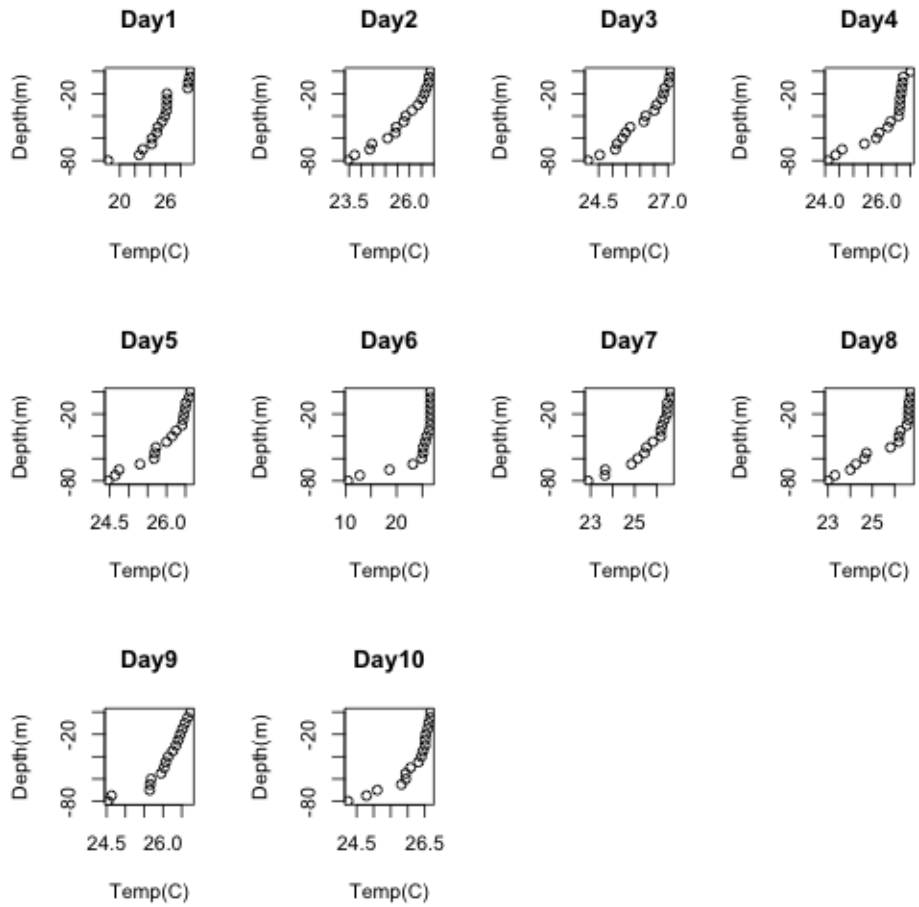


Figure 1: Temperature and depth data recorded by a PTT-100 HR PSAT (Microwave Telemetry, Columbia, MD) attached to swordfish 61665. The raw data were interpolated and averaged at every 20 m depth to a maximum depth of 660 m.

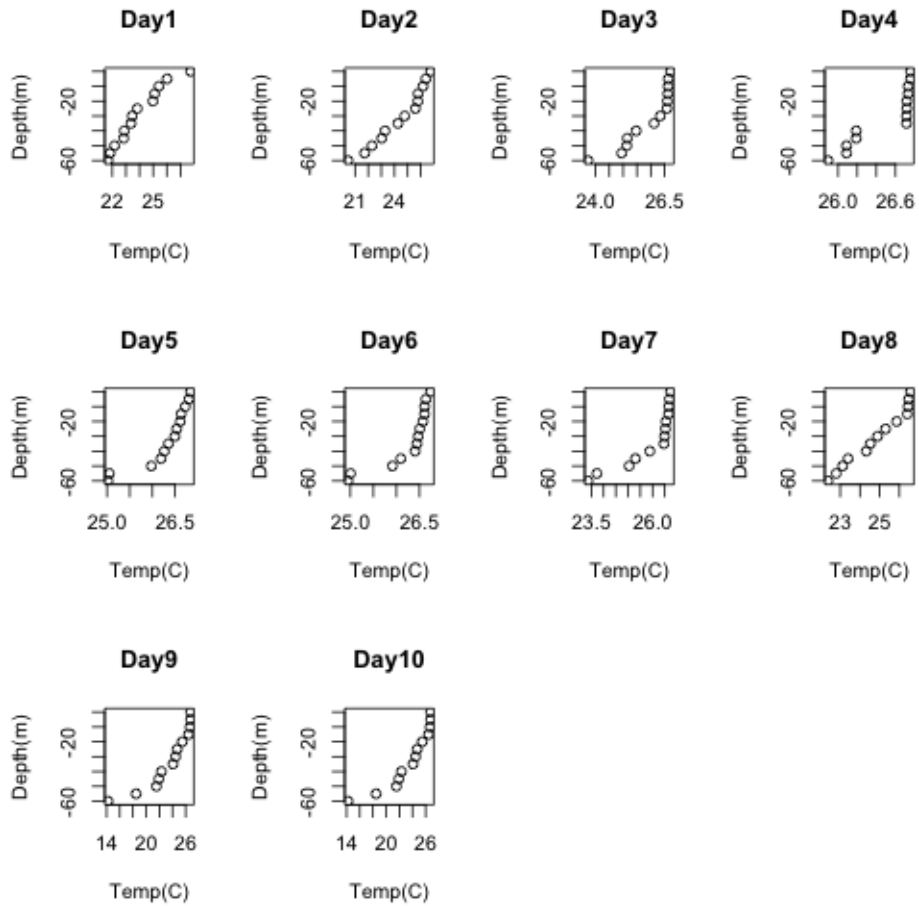
Figures 2.



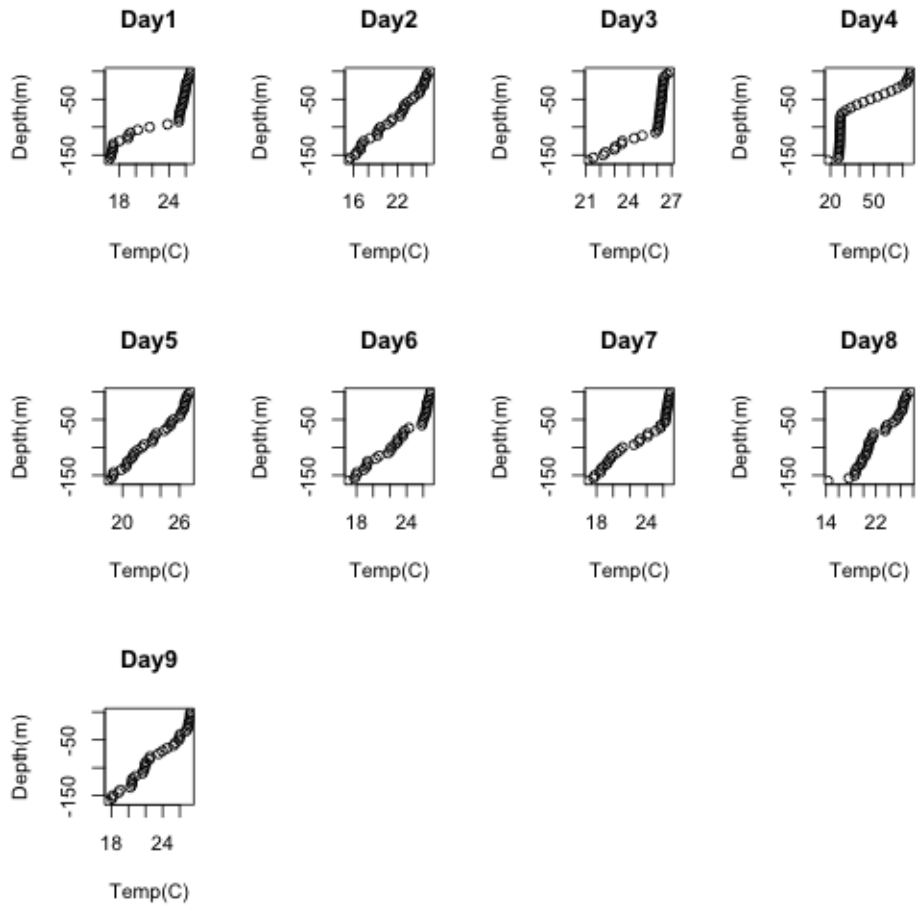
a) Blue marlin #41333



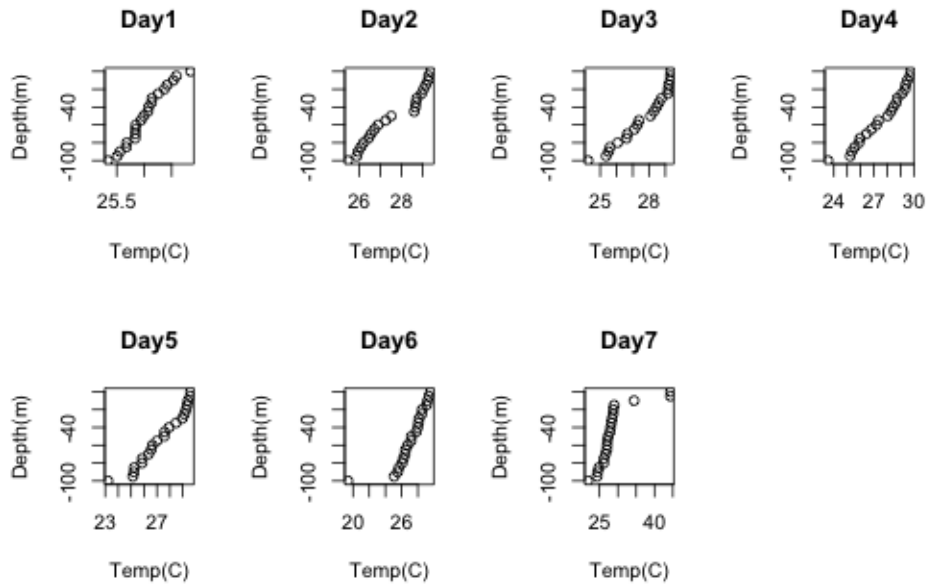
b) Blue marlin #24523



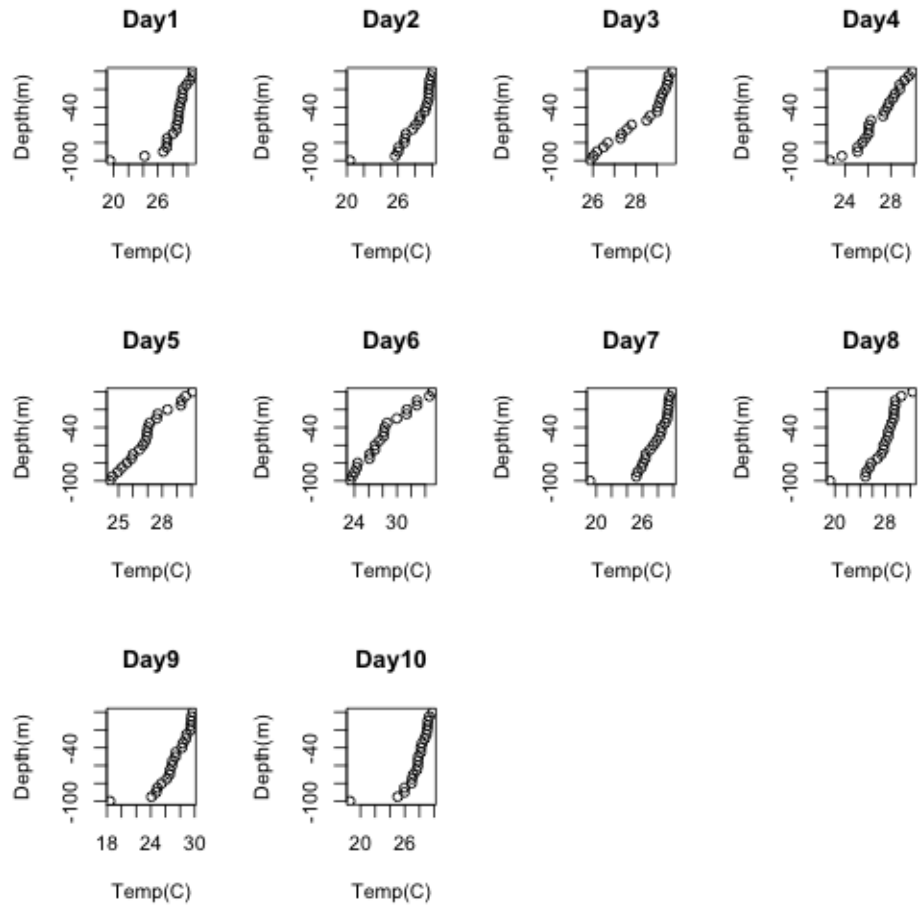
c) Blue marlin #34233



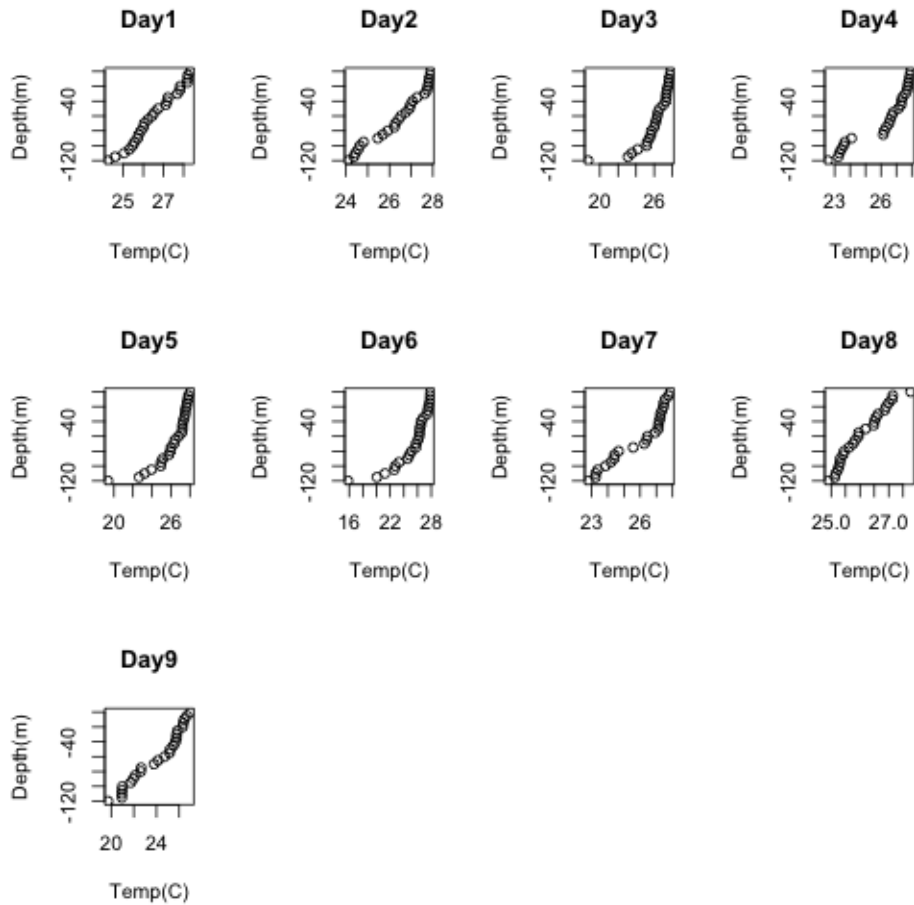
d) Blue marlin #59080



e) Blue marlin #84351



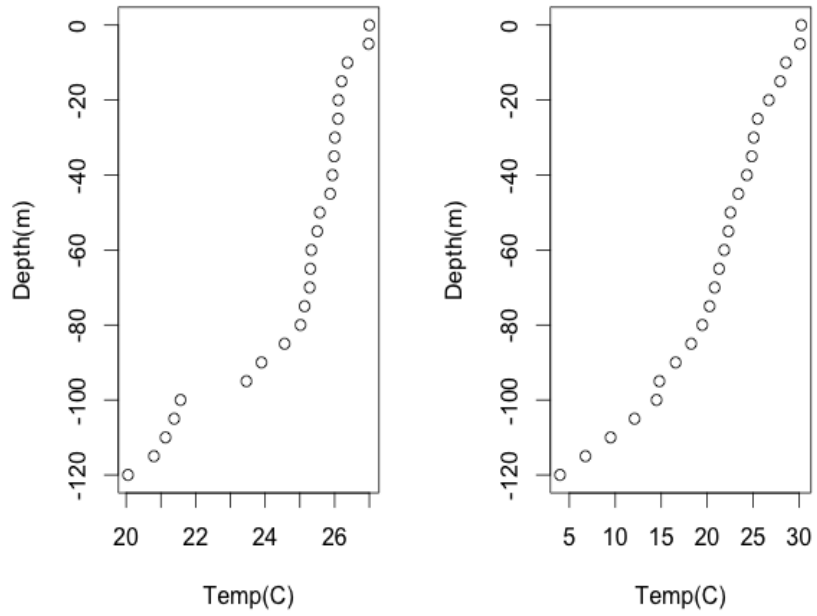
f) Blue marlin #84363



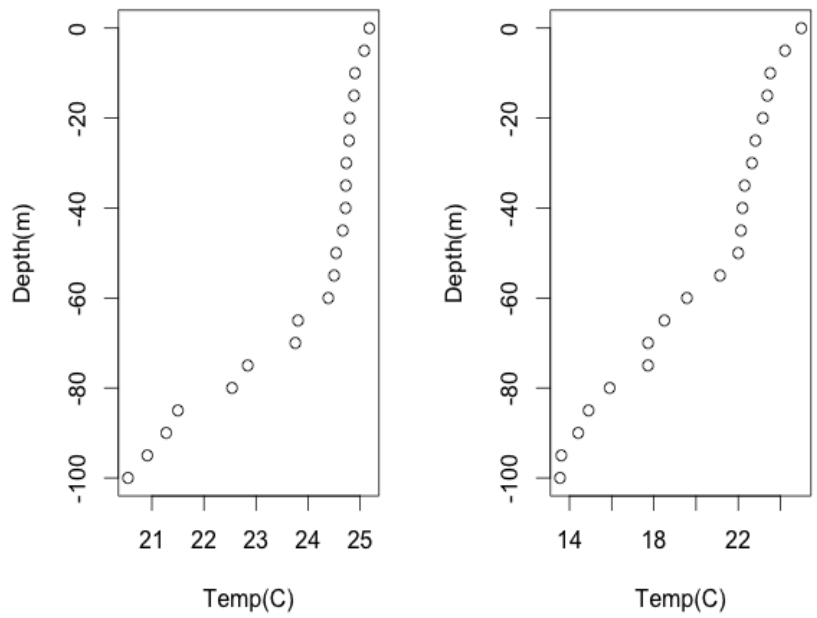
g) Blue marlin #35687

Figures 2: Daily temperature profiles recreated using Microwave Telemetry, Inc. model PTT-100 tags deployed on blue marlin (n=7) interpolated and averaged at every 5 m depth.

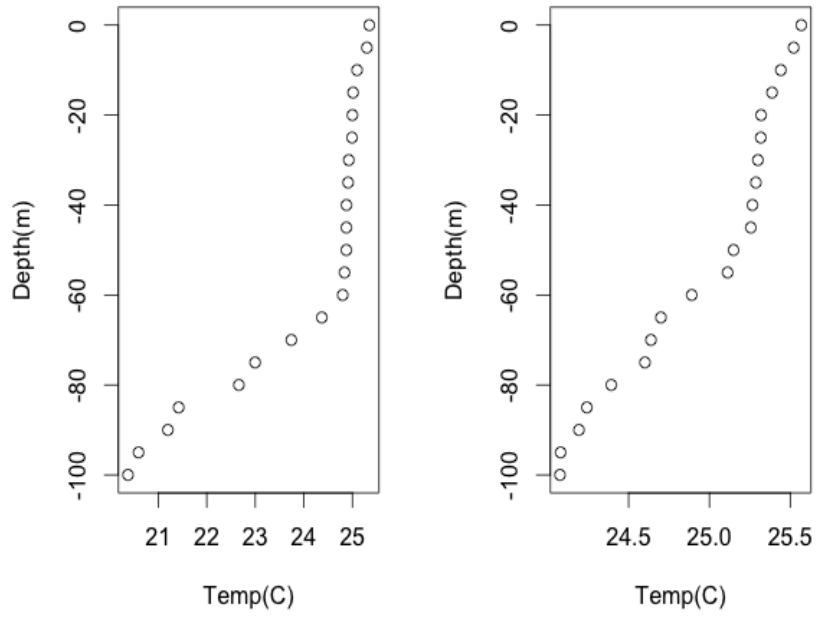
Figures 3.



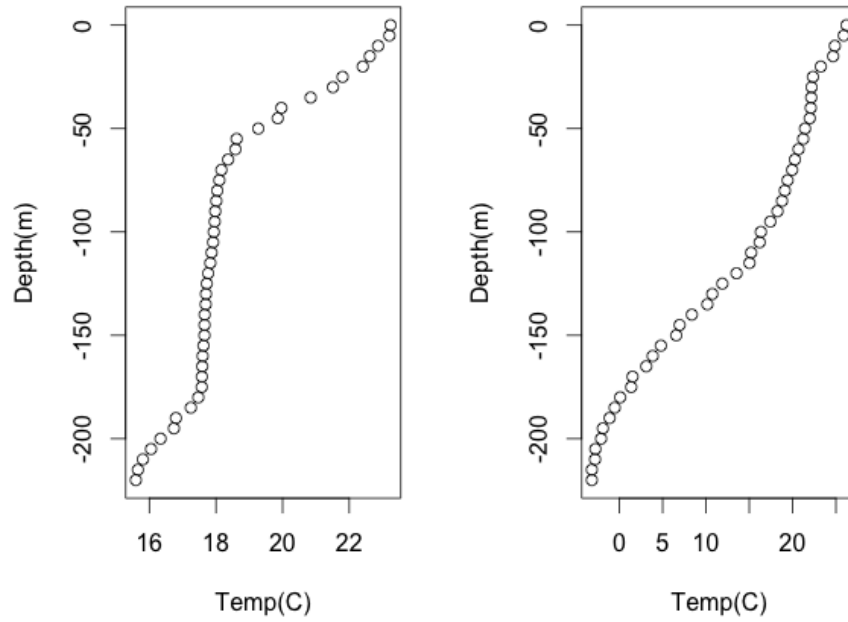
a) Blue marlin #112321



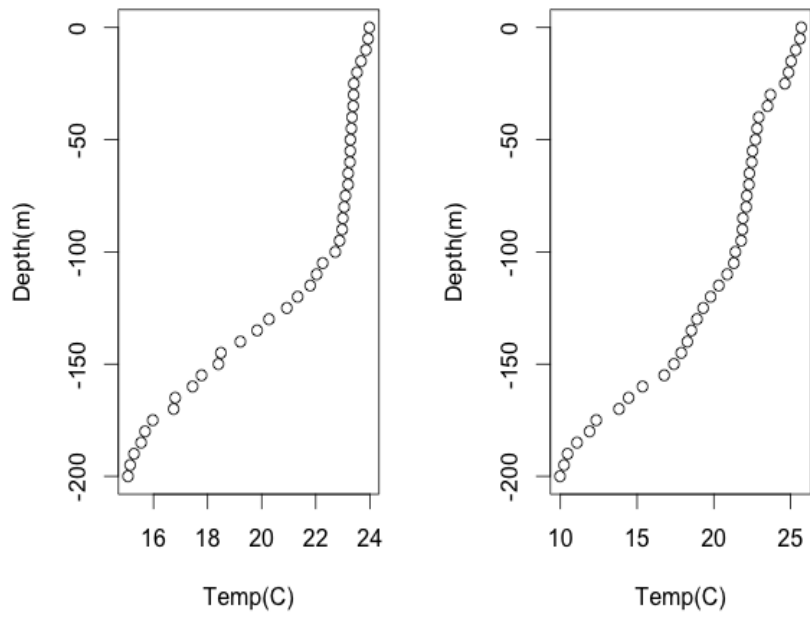
b) *Black marlin #111218*



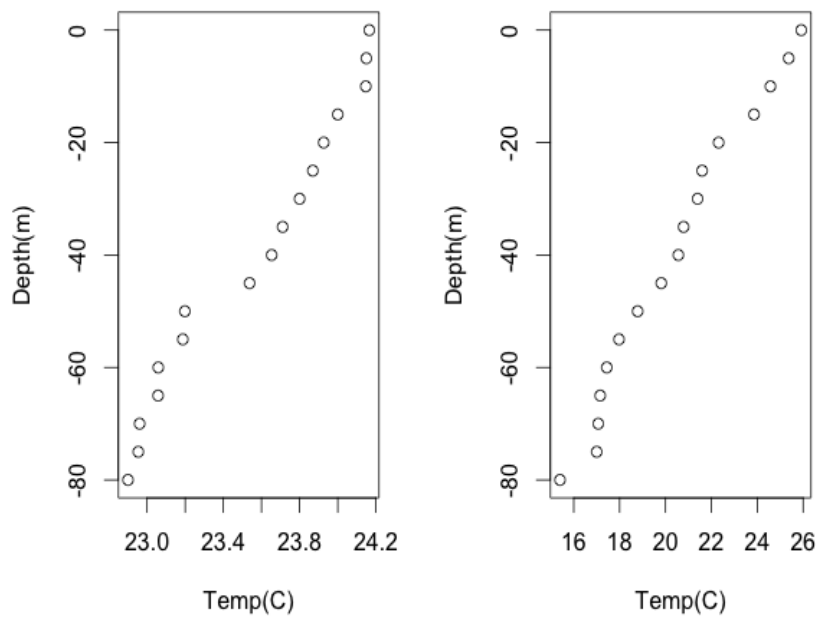
a) *Blue marlin #111213*



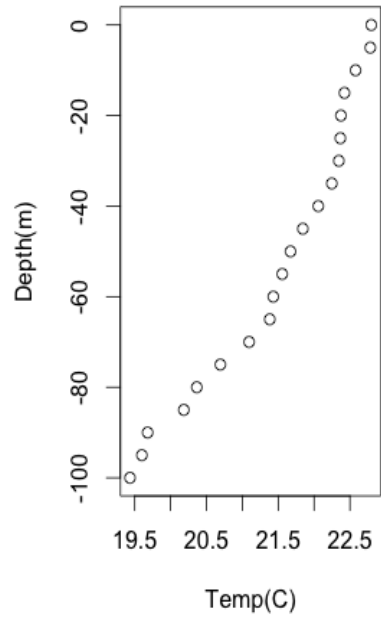
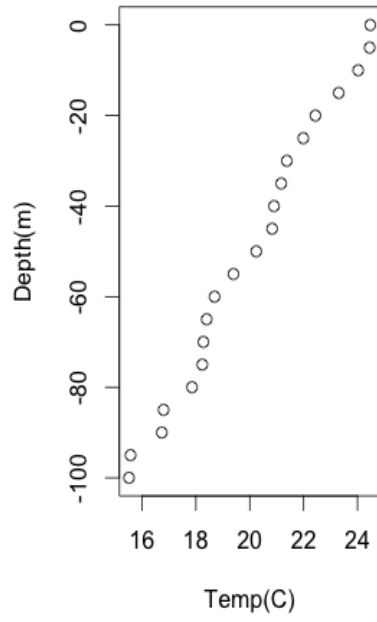
b) *Blue marlin #112322*



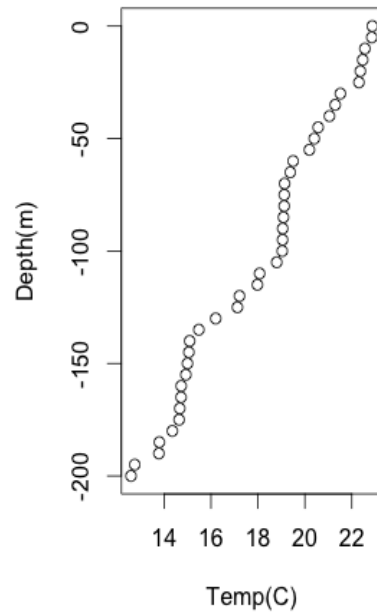
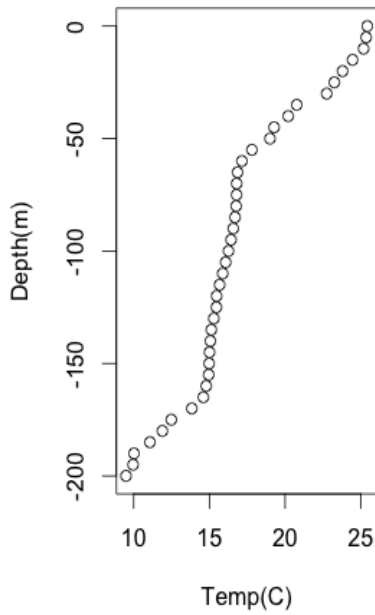
c) *Blue marlin #112320*



d) *Blue marlin #112323*



e) *White marlin #126323*



f) *White marlin #126288*

Figures 3. Temperature profiles recreated for the initial (left) and final (right) day of tagging using data from Wildlife Computers, Inc. model Mk10 PATs deployed on blue, white, and black marlin (n=9).

where X is longitude and Y is latitude and $i = \text{day } 1, 2 \dots n$. Linearity is assumed in PCA due to our reliance on the original data to interpolate between individual data points. A bilinear system is applied to calculate the resulting coordinates as simply as possible. Therefore, we assume both longitude and latitude change linearly with PC value, so that:

$$X_i = aPC_{i,1} + b$$

$$Y_i = cPC_{i,1} + d$$

Each set of coefficients (a, b) and (c, d) are found by using the initial and final location. These coefficients represent the change in longitude (a, b) and latitude (c, d) over time as determined by the dominant vector pattern (PC1) of days 1 and n .

$$\begin{matrix} a \\ b \end{matrix} = \begin{bmatrix} PC_{1,1} & 1 \\ PC_{n,1} & 1 \end{bmatrix}^{-1} \begin{matrix} X_1 \\ X_n \end{matrix}$$

$$\begin{matrix} c \\ d \end{matrix} = \begin{bmatrix} PC_{1,1} & 1 \\ PC_{n,1} & 1 \end{bmatrix}^{-1} \begin{matrix} Y_1 \\ Y_n \end{matrix}$$

Error Metric

In addition to data archived by the Kerstetter Fisheries Laboratory, data used in the comparison analyses were donated by John Graves (Virginia Institute of Marine Science, College of William & Mary) and Andrij Horodysky (Hampton University), as well as the IGFA via partnering with researchers from Stanford University. Light-based geolocation coordinate estimates were generated using two separate state-space models. Microwave Telemetry tags were deployed on blue marlin as part of a previous tagging study (Graves and Horodysky 2010). The light records were formatted in a centralized tag database computer program, *Tagbase*, (Lam and Tsonotos 2011) before being imported into R. The light data were run through the *TrackIt* model to generate light-based coordinate estimates.

Wildlife Computers Mk10 and MiniPATs were deployed on blue, black, and white marlin as part of the International Game and Fishing Association (IGFA) International Great Marlin Race (IGMR). A “best fit” track was created courtesy of

IGFA and Stanford University. First, an initial track was generated using the Wildlife Computers WC-GPE2 software and light data to derive longitude. SST data were then added to derive latitude. This track was then put through a state-space model that uses a sophisticated algorithm to establish the “best fit” estimates (IGFA 2013).

The root mean square estimation (RMSE) is calculated by finding the difference between the daily latitude and longitude estimates.

For each day j ,

$$\Delta\text{lat} = X_{j(\text{geu})} - X_{j(\text{PCA})}$$

$$\Delta\text{lon} = Y_{j(\text{geu})} - Y_{j(\text{PCA})}$$

$$^c \text{Latitude } (C_x) = 111.12\text{km}$$

$$^c \text{Longitude } (C_y) = 111.12 \cos(\text{lat})$$

$$\text{RMSE} = \frac{1}{\sqrt{(\Delta\text{lat}_j \times C_x)^2 + (\Delta\text{lon}_j \times C_y)^2}}$$

All model statistical computations were performed in R software environment. All coordinate estimates given by both light-based models and the PCA model were imported and organized in Excel files. A tag summary table was created compiling all information regarding tag deployments and resulting error calculations (Tables 1). Error calculations within 1 degree, roughly 111km, were considered “good,” and those within 2 degrees (222km) considered “reasonable.” For each tag deployment, error calculated each day was plotted over time to determine any trends (Figures 6a-h). These RMSE values were then averaged over the course of the tagging duration (Table 2), and plotted over total days at large to determine any correlation (Figure 7).

Each track was plotted in R using a map function (package ‘rworldmap’). Maps created from the light-based estimates and PCA model estimates were placed side-by-side for a visual comparison (Figures 5a-h). The simple plot function was used for the short deployments (e.g. 9-10 days) where the light-based estimates derived by *TrackIt* were overlaid onto the PCA model estimates (Figures 4a-g). Estimates given for the swordfish data plotted in R. Maps were created in ‘GoogleEarth’ using satellite imagery to visualize movement among topographic features (Figures 9a-d).

Table 1: Species code, tag ID number, tag manufacturer (MT = Microwave Telemetry, WC = Wildlife Computers), tag model, region, total days at large (DAL), track duration (where sufficient data was provided for both analyses), initial and final coordinates, net displacement (ND).

Species Code	Tag ID	Tag Man.	Tag Model	Region	DAL	Track Duration	Initial Lat.	Initial Lon.	Final Lat.	Final Lon	ND
BUM	41333	MWT	PTT100	VZ	10	3/17/08 - 3/27/08	10.87N	67.14W	11.7N	68.28W	139
BUM	24523	MWT	PTT100	VZ	10	5/15/08 - 5/25/08	10.97N	66.97W	11.05N	67.03W	10
BUM	34233	MWT	PTT100	VZ	10	5/17/08 - 5/27/08	10.72N	67.17W	11.47N	66.8W	87
BUM	59080	MWT	PTT100	VZ	9	4/18/09 - 4/27/09	11.0N	67.05W	11.73N	66.59W	96
BUM	84351	MWT	PTT100	VI	10	9/11/08 - 9/21/08	18.7N	64.8W	18.2N	62.75W	197
BUM	84363	MWT	PTT100	VI	10	9/30/09 - 10/10/09	18.72N	64.78W	20.57N	66.38W	271
BUM	35687	MWT	PTT100	NC	10	6/22/08 - 7/2/08	35.07N	75.57W	38.05N	65.38W	943
BUM	111212	WC	Mk10	ZA	72	2/25/12 - 4/30/12	30.75S	31.4E	27.31S	34.4E	322
BUM	112321	WC	Mk10	ZA	32	3/30/12 - 4/25/12	29.25S	34.2E	26.12S	35.5E	558
BUM	111213	WC	Mk10	ZA	120	5/6/12 - 8/28/12	27.08S	33.6E	25.47S	34.8E	170
BLM	111218	WC	Mk10	ZA	120	5/3/12 - 8/28/12	28.71S	32.9E	25.99S	33.8E	413
BUM	112322	WC	Mk10	POR	28	8/4/12 - 8/27/12	17.1S	32.76E	15.2S	32.18E	183
BUM	112320	WC	Mk10	POR	90	8/12/12 - 11/4/12	17.4S	30.45E	24.0S	22.62E	2263
BUM	112323	WC	Mk10	POR	81	8/26/13 - 11/7/13	18.2S	32.67E	13.0S	34.68E	676
WHM	126323	WC	MiniPAT	MR	32	10/15/13 - 11/5/13	9.1S	37.56E	18.3S	28.62E	1819
WHM	116288	WC	Mk10	MR	47	10/15/13 - 11/11/13	7.0S	34.4E	14.5S	35.31E	889
SWO	61669	MWT	PTT100	FL	10	12/16/11 - 12/26/11	26.77N	79.76W	30.81N	75.21W	58
SWO	86995	MWT	PTT100	CZ	10	4/1/12 - 4/10/12	19.8N	79.24W	20.42N	78.93W	77
SWO	61665	MWT	PTT100	CZ	10	4/21/13 - 4/30/13	19.8N	79.22W	19.83N	79.23W	63
SWO	88095	MWT	PTT100	CZ	30	4/12/14 - 5/13/14	19.80N	79.23W	19.6N	78.63W	68

Table 2. Species code, tag ID number, tag manufacturer (MT = Microwave Telemetry, WC = Wildlife Computers), tag model averaged root mean square error (RMSE) calculated each day of tag duration (in km), max depth (MD) recorded by tag (in m), average depth (AD) as recorded by tag (in m)

Species Code	Tag ID	Tag Model	RMSE	Max Depth	Avg. Depth
BUM	41333	PTT100	75.88	-356	-15
BUM	24523	PTT100	3.52	-156	-14
BUM	34233	PTT100	31.47	-87	-7
BUM	59080	PTT100	27.69	-237	-22
BUM	84351	PTT100	50.27	-254	-30
BUM	84363	PTT100	176.14	-326	-21
BUM	35687	PTT100	130.02	-323	-28
BUM	111212	Mk10	370.38	-216	-38
BUM	112321	Mk10	284.74	-192	-38
BUM	111213	Mk10	245.36	-208	-39
BLM	111218	Mk10	213.47	-216	-38
BUM	112322	Mk10	133.50	-224	-54
BUM	112320	Mk10	381.01	-336	-62
BUM	112323	Mk10	251.90	-336	-60
WHM	126323	MiniPAT	251.72	-208	-55
WHM	116288	Mk10	161.20	-248	-59
SWO	61669	PTT100	N/A	-506	-218
SWO	86995	PTT100	N/A	-651	-357
SWO	61665	PTT100	N/A	-756	-308
SWO	88095	PTT100	N/A	-597	-295

RESULTS

Comparison Analyses

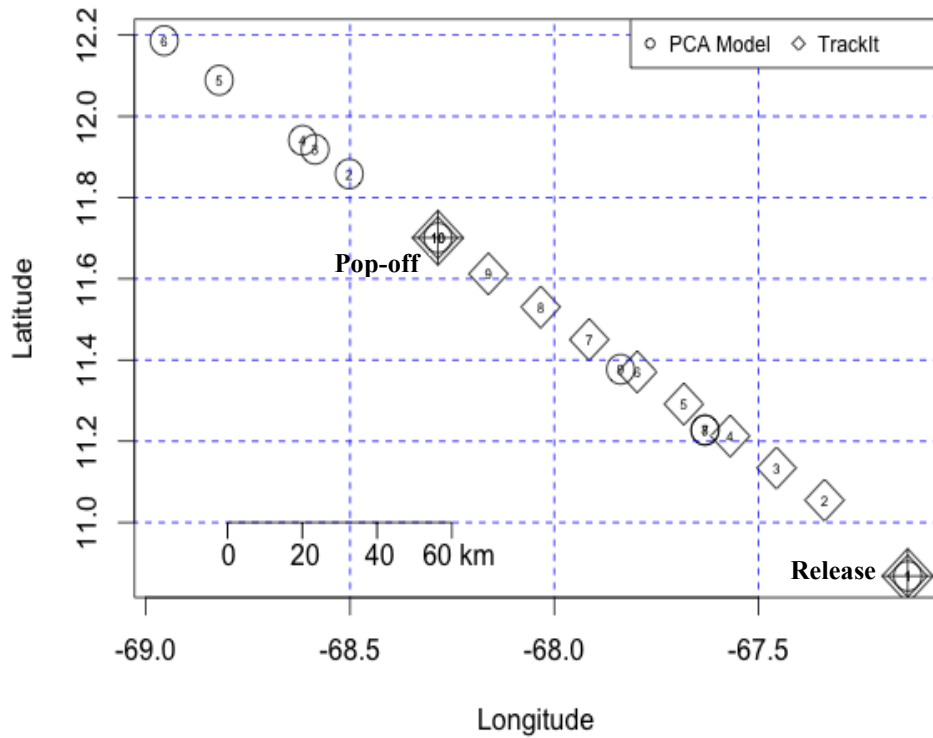
A total of 16 comparisons were made using data from Microwave Telemetry PTT-100 HR PSATs and Wildlife Computers PATs (Mk10, MiniPAT) deployed on blue, black, and white marlin (Figures 4 and 5). Root mean square error (RMSE) values calculated each day showed the average error of our model to be 174.3 km with a standard deviation of 118.9 km. RMSE calculated each day were plotted over time for each deployment, although these plots did not reveal any significant trends in our results (Figures 6a-f).

Light data from seven PTT-100 HRs deployed on blue marlin was run through *TrackIt* to generate a light-based “best fit” track. The comparison to the PCA generated estimates yielded an average error of 70.7 km with a standard deviation of 61.9 km. Data from a total of nine Mk10s and MiniPATs deployed on blue marlin (n=6), white marlin (n=2) and black marlin (n=1) were used in a separate comparison. The “best fit” track created from these tags used a state space model that incorporated satellite SST. RMSE calculations from the *TrackIt* model and SST model revealed an error of 70.7 km and 254.8 km respectively (Table 3).

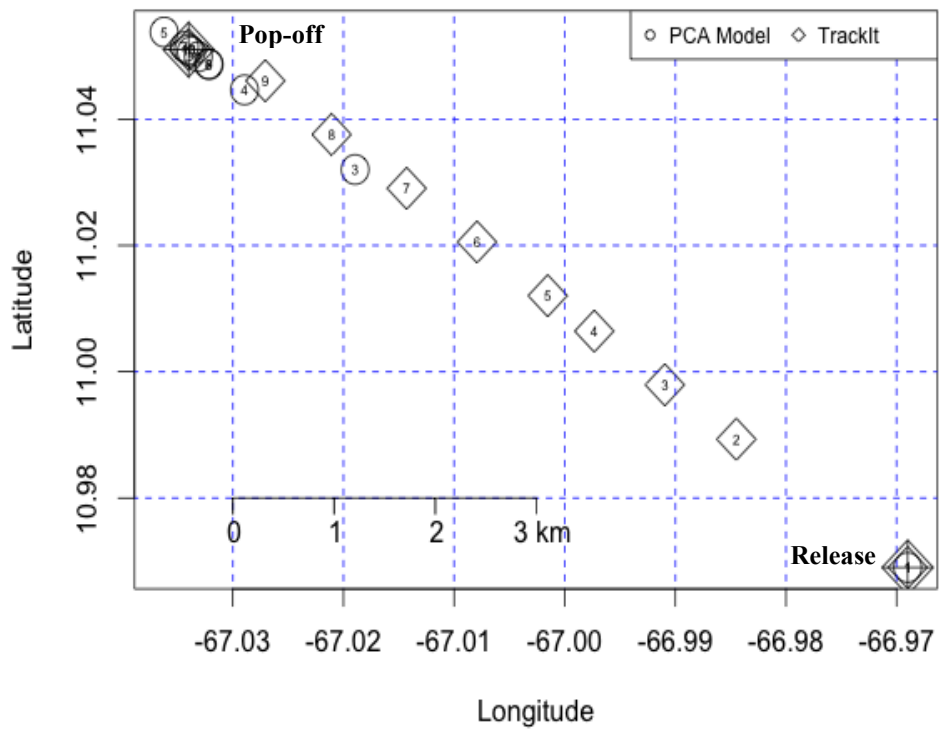
Swordfish Projections

Four tracks were made from swordfish tagged and released in the Caribbean Sea near the Cayman Islands (n=3) and in the Florida Straits (n=1) (Figures 8a-d). Estimates derived from our model demonstrate swimming behavior that is supported by previous swordfish tagging studies. The swordfish released in the Northwest Atlantic show a northward movement towards the “Charleston Bump” located on the Blake Plateau, just east of the South Carolina and Georgia coastline (Figure 8a). Trips to the Charleston Bump are strongly supported by previous tagging studies that suggest that this productive region is a possible semi-resident feeding ground for immature swordfish (Sedberry and Loefer 2001).

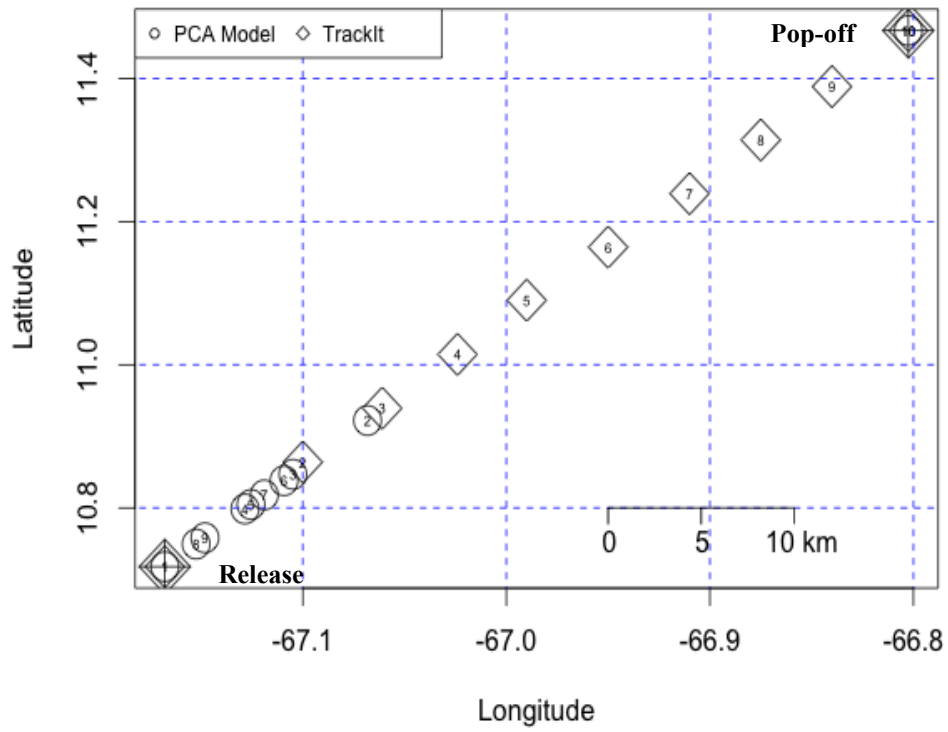
Figures 4.



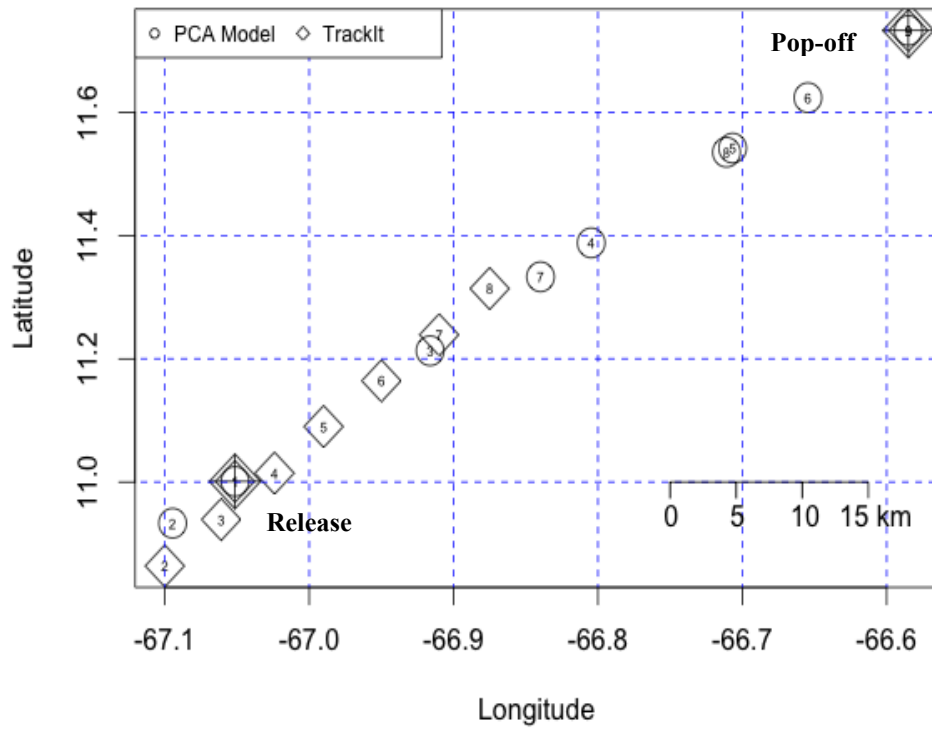
a) BUM 41333; Caracas, VZ, March 17, 2008 – March 27, 2008



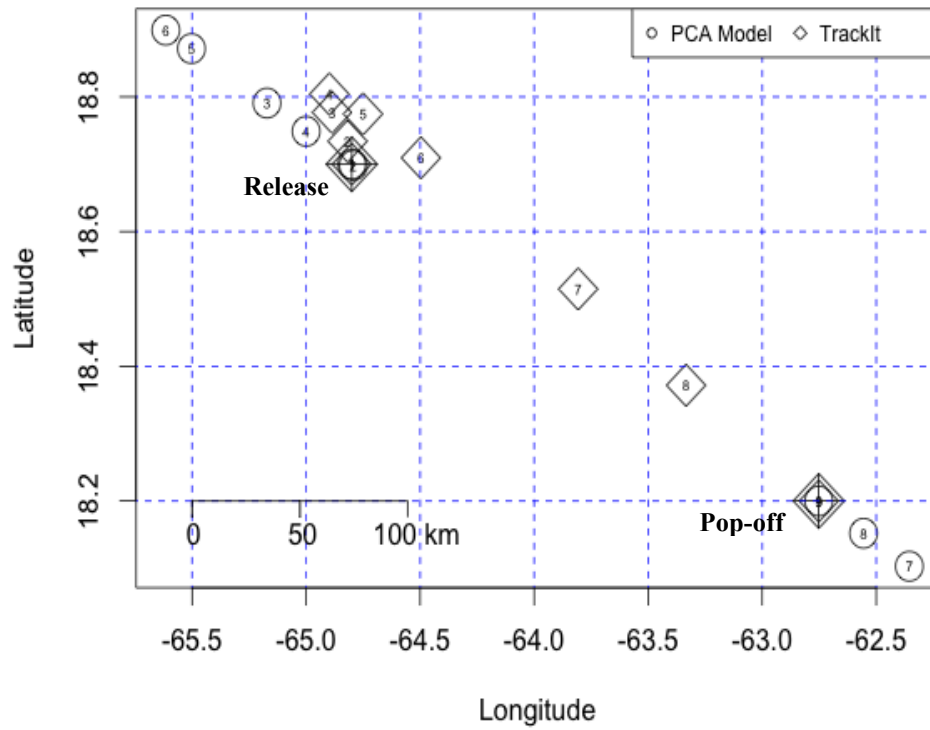
b) BUM 24523; Caracas, VZ, May 15, 2008 – May 25, 2008



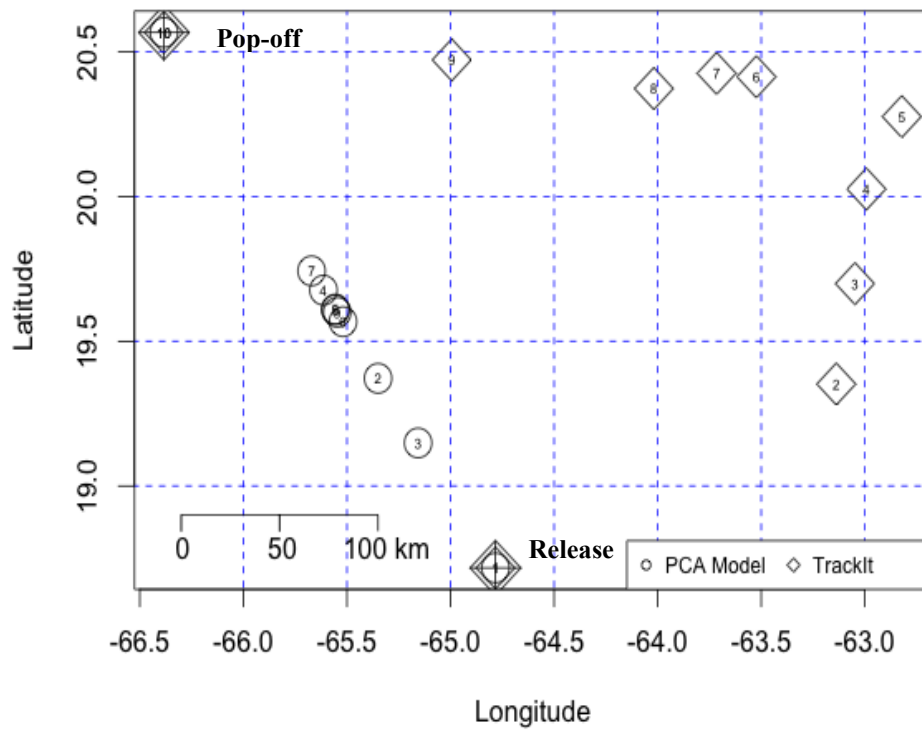
c) BUM 34233; Caracas, VZ, May 17, 2008 – May 27, 2008



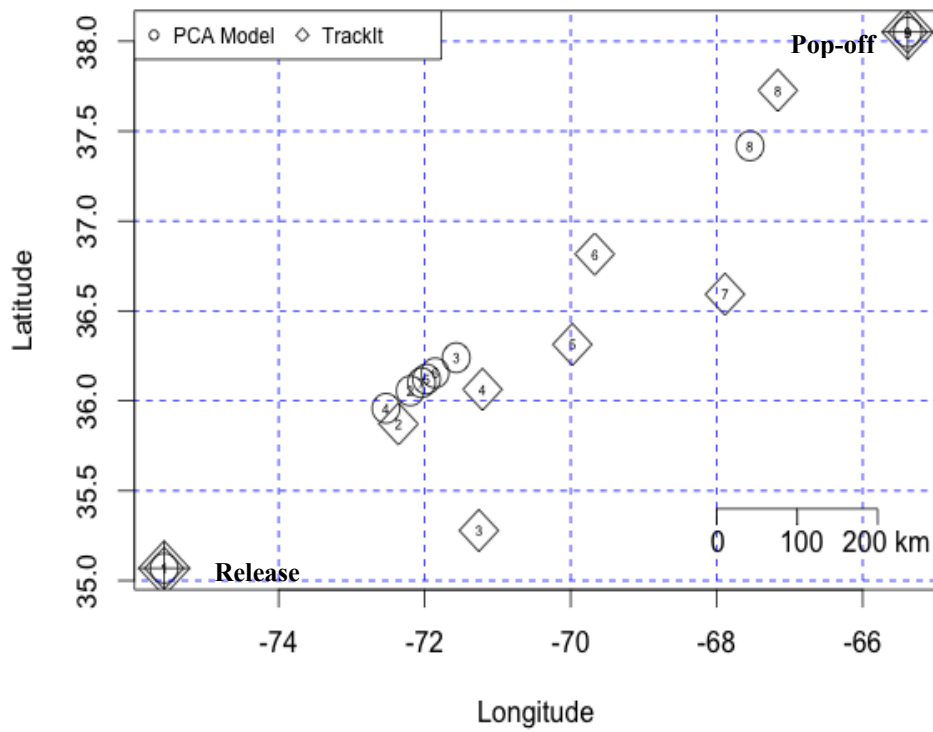
d) BUM 59080; Caracas, VZ, April 18, 2009 – April 27, 2009



e) BUM 84351; Virgin Islands, September 11, 2008 – September 21, 2008



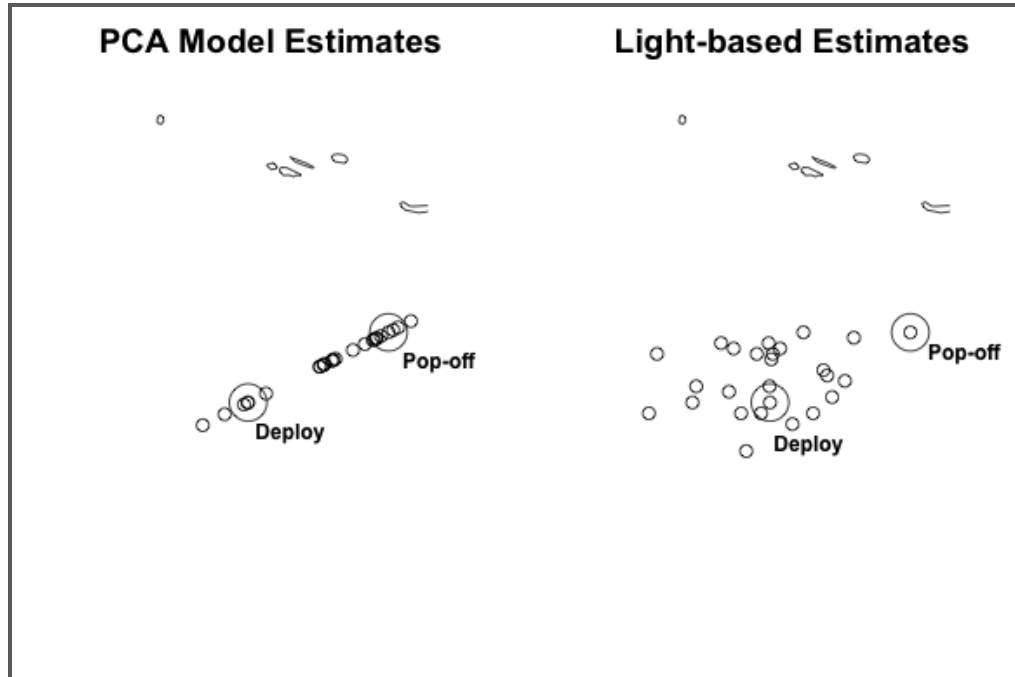
f) BUM 84363; Virgin Islands, September 30, 2009 – October 10, 2009



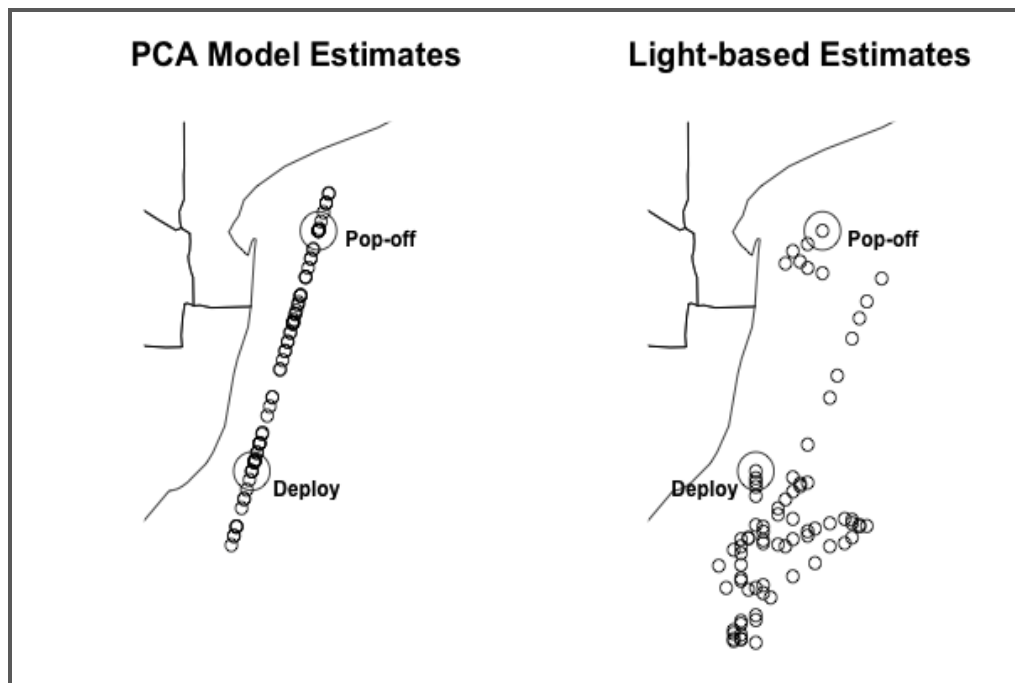
g) BUM 35687; Florida Straits, June 22, 2008 – July 2, 2008

Figures 4. Estimates of marlin tagged with Microwave Telemetry, Inc. model PTT-100 tags (n=7) as given by the hydrographic PCA model and the light-based model, *TrackIt*. The locations of fish release and final tag pop off are highlighted.

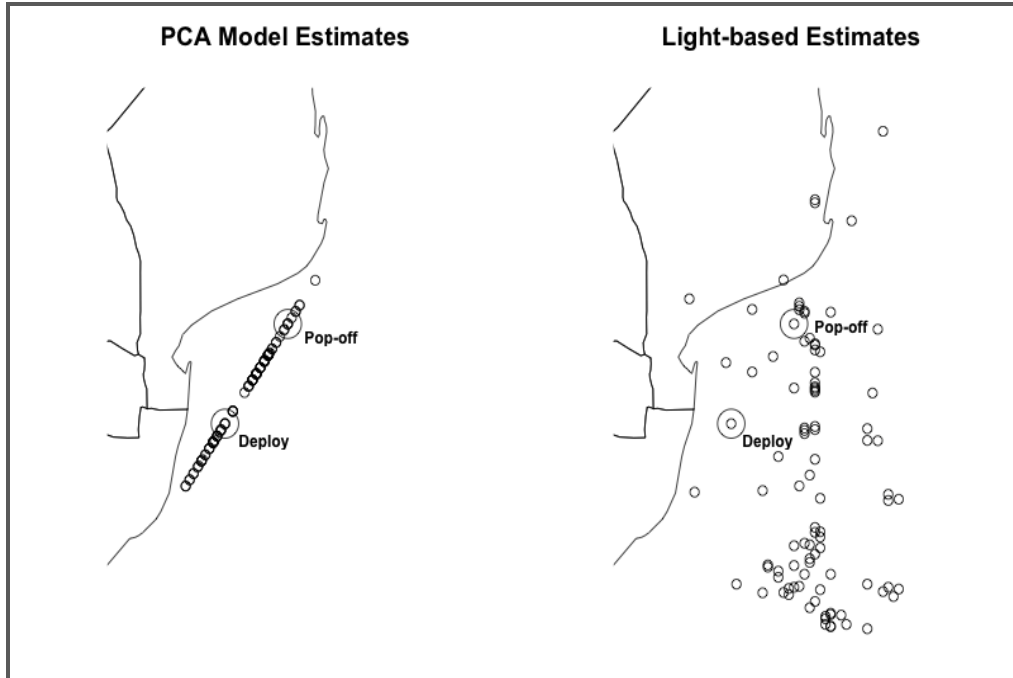
Figures 5.



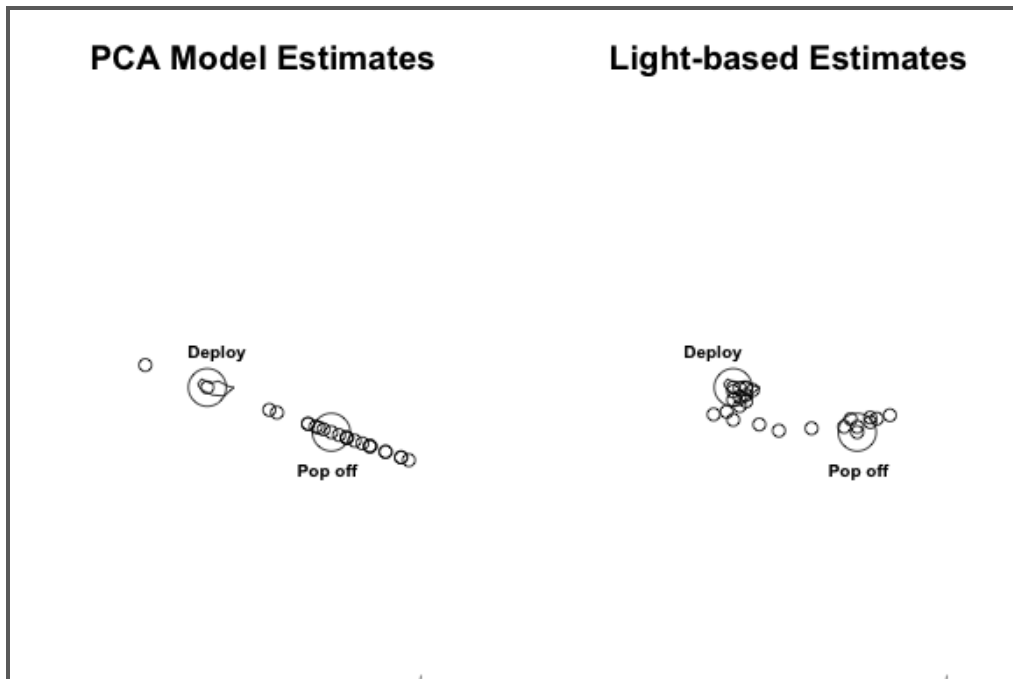
a) Blue marlin #112321; South Africa March 30, 2012 – April 25, 2012



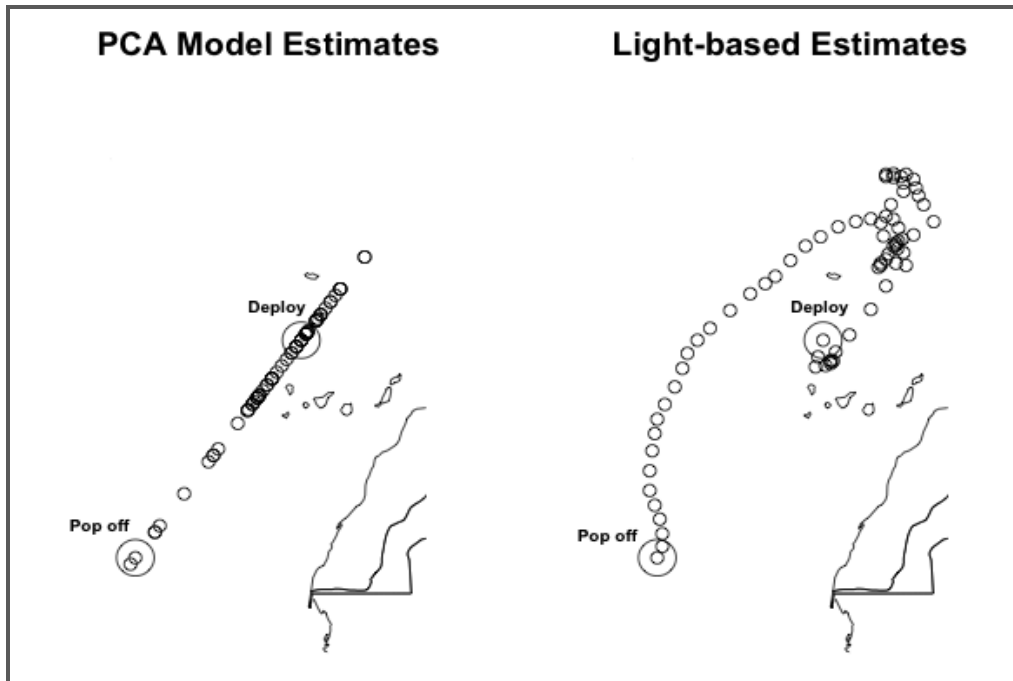
b) Black marlin #111218; Richard's Bay, South Africa May 3, 2012 – August 28, 2012



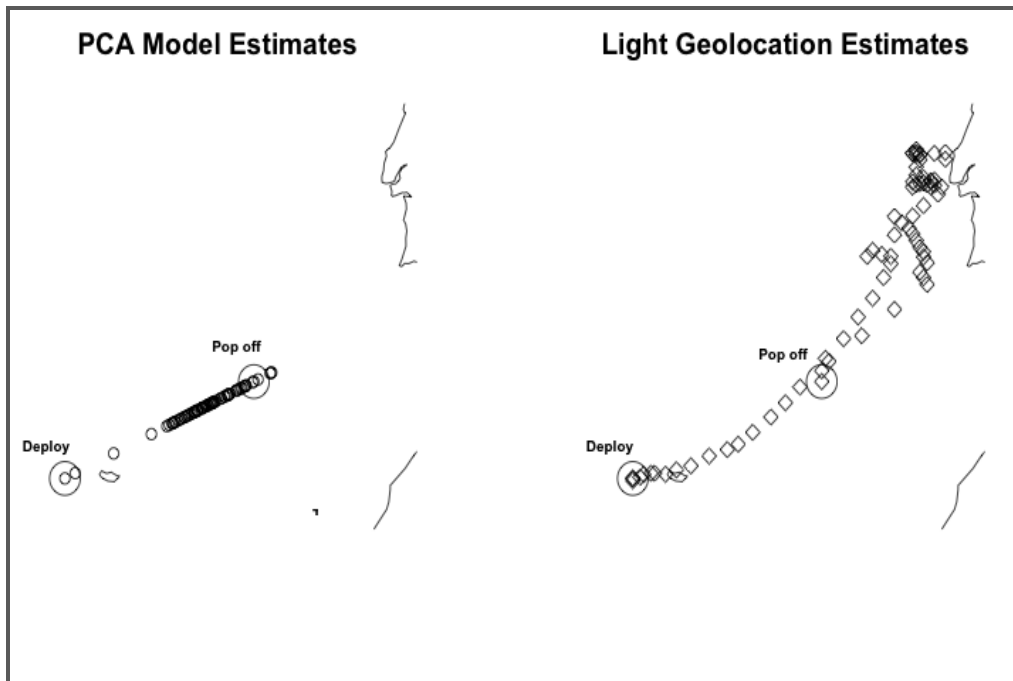
c) Blue marlin #111213; Richard's Bay, South Africa May 6, 2012 – August 28, 2012



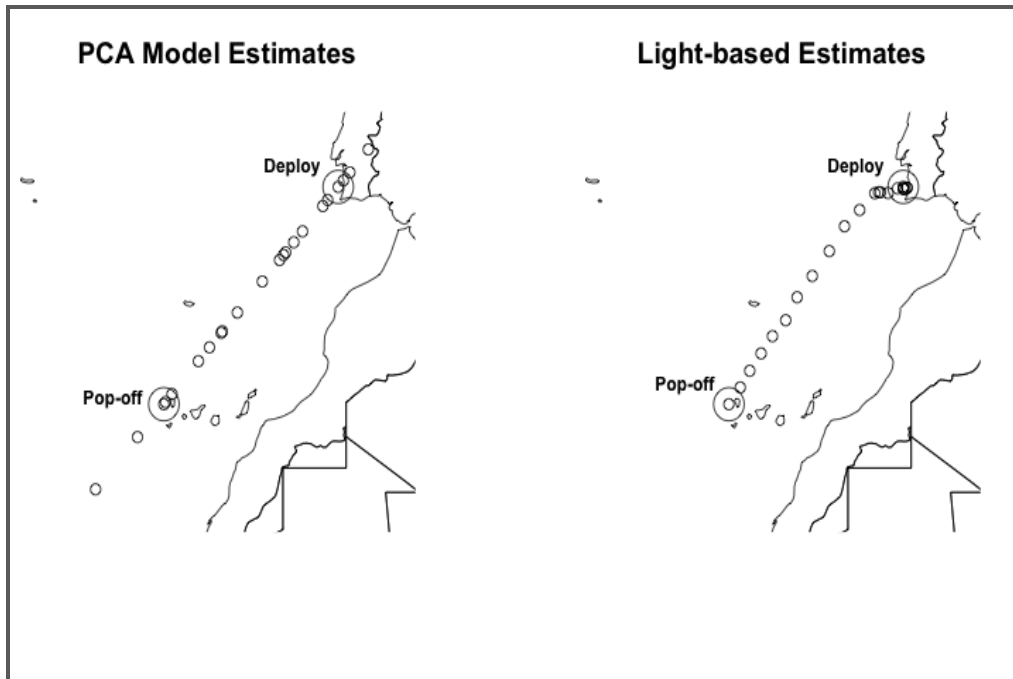
d) Blue marlin #112322; Madeira, POR, August 4, 2012 – August 27, 2012



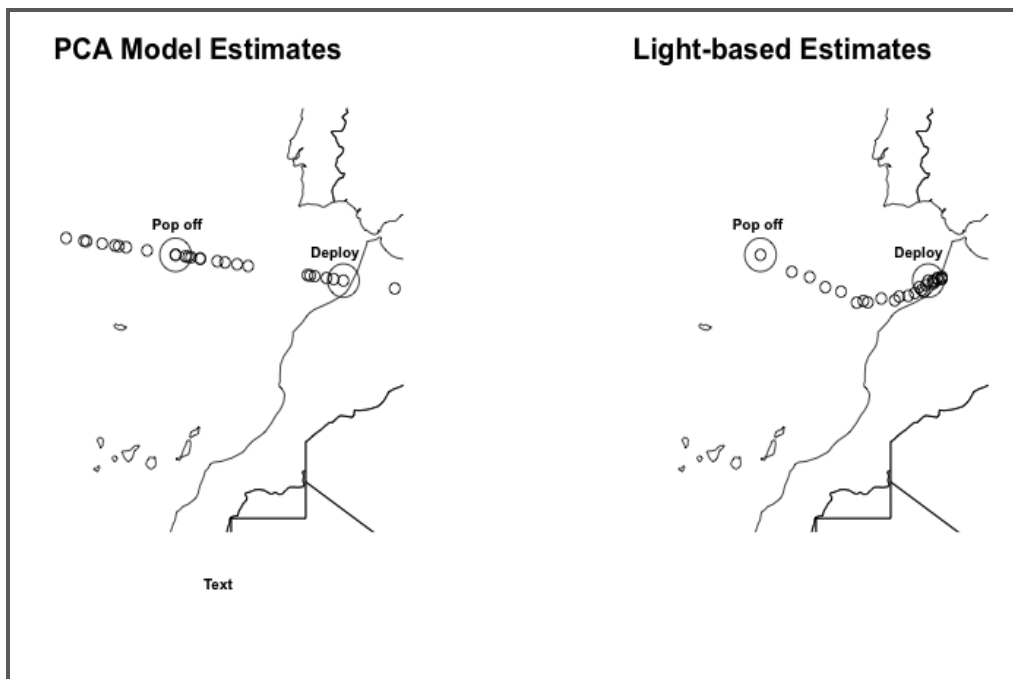
e) Blue marlin #112320; Madeira, POR, August 12, 2013 – November 4, 2012



f) Blue marlin #112323; Madeira, POR, August 26, 2013 – November 7, 2012

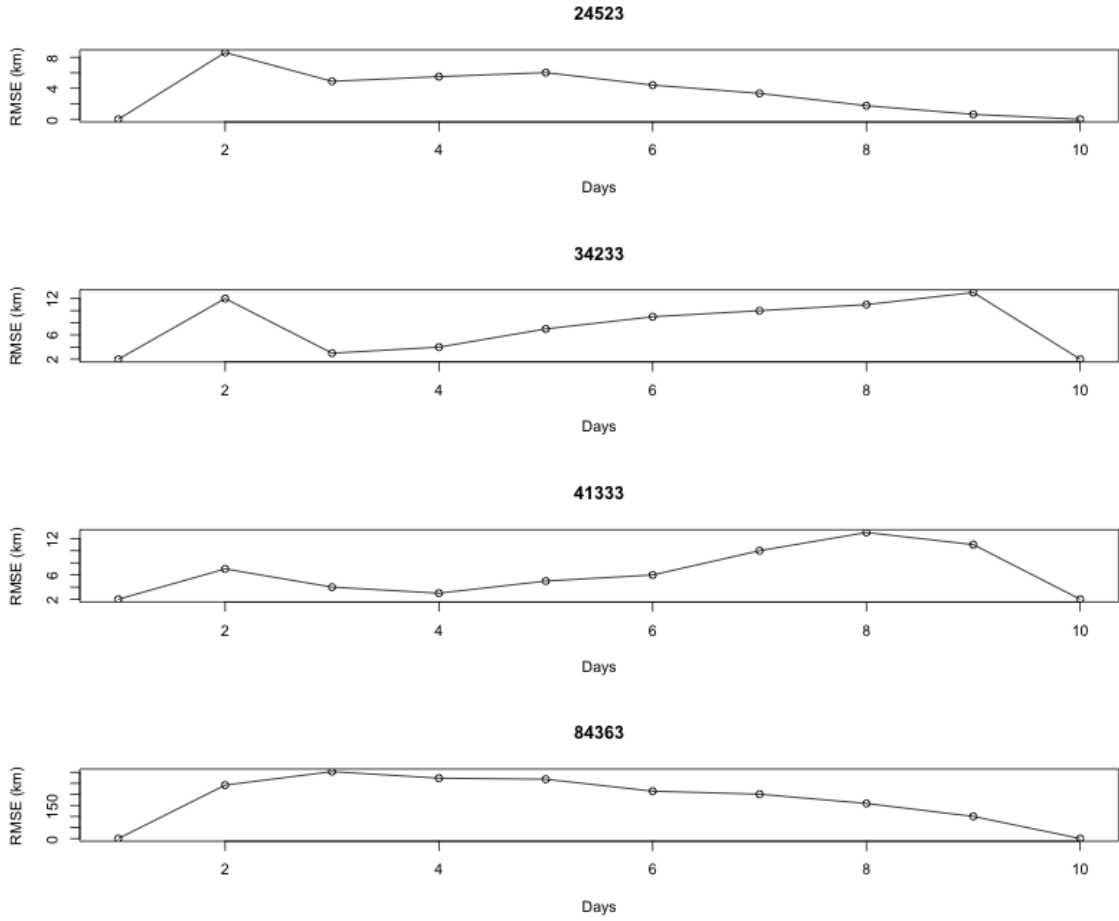


g) White marlin #126323; Morocco, October 15, 2013 – November 5, 2013

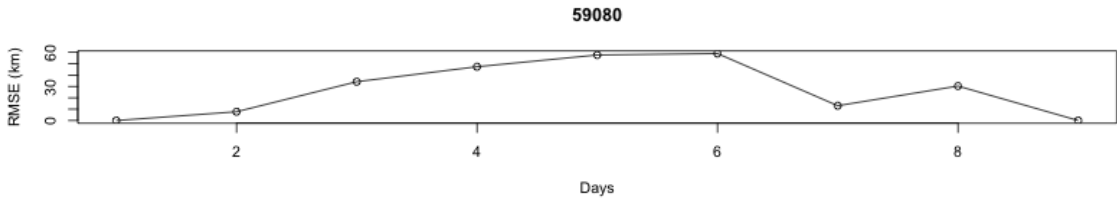
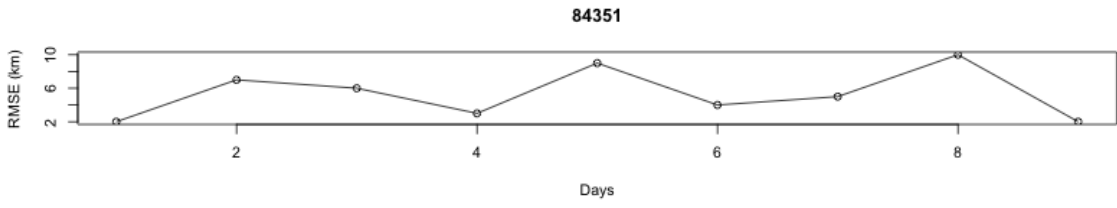


h) White marlin #126288; Morocco, October 15, 2013 – November 11, 2013

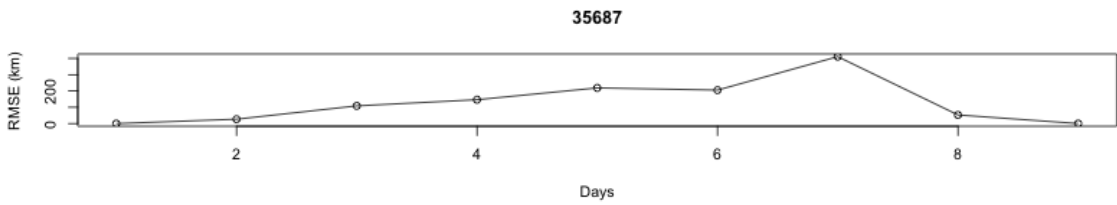
Figures 5. Coordinate estimates of marlin tagged with Wildlife Computers, Inc. model Mk10 PATs (n=9). On the left is the track derived from the hydrographic PCA model, while on the right are the estimates from a light-based state-space model that uses the tag's raw global positioning estimates and incorporates satellite sea-surface temperature (SST).



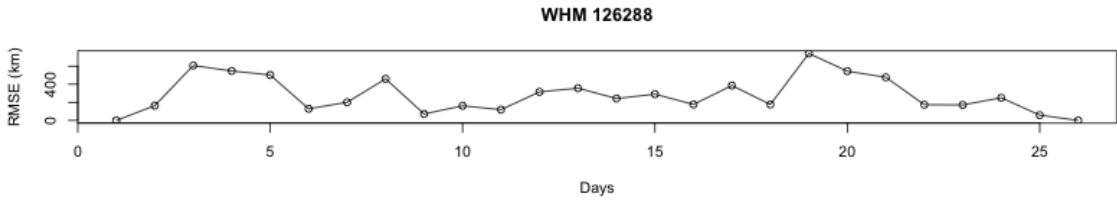
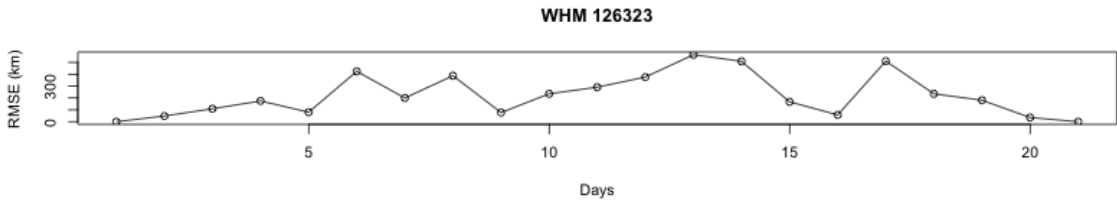
a) Caracas, Venezuela, 2008.



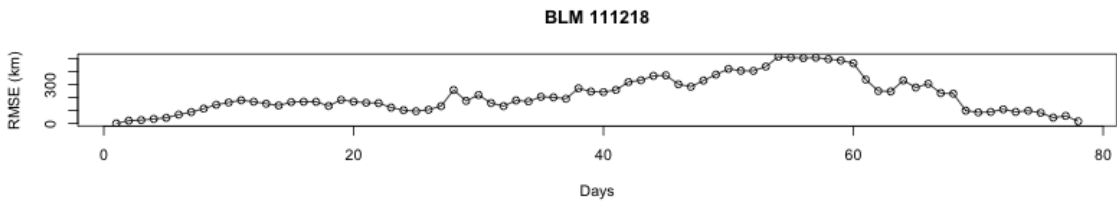
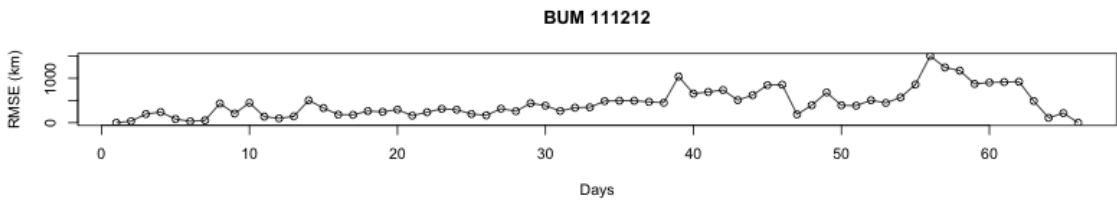
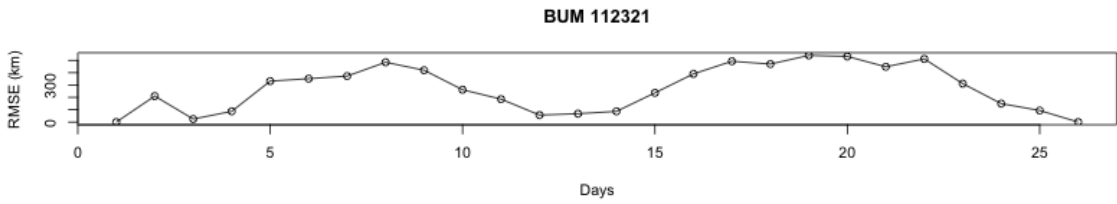
b) British Virgin Islands, 2008 and 2009.



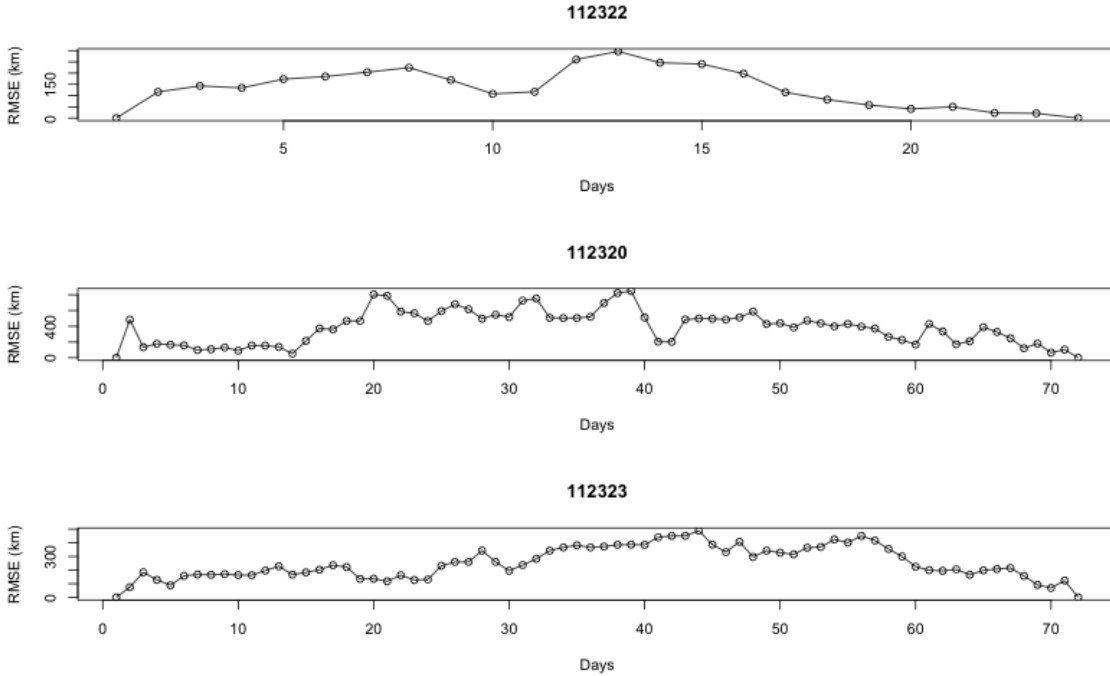
c) North Carolina, 2008.



d) Mohammedia, Morocco, 2012.



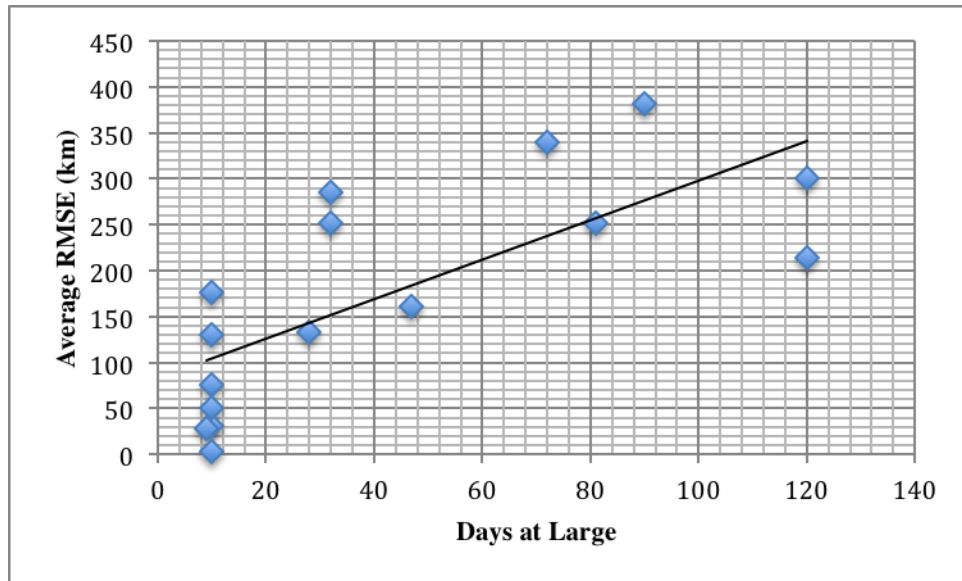
e) Richard's Bay, South Africa, 2012.



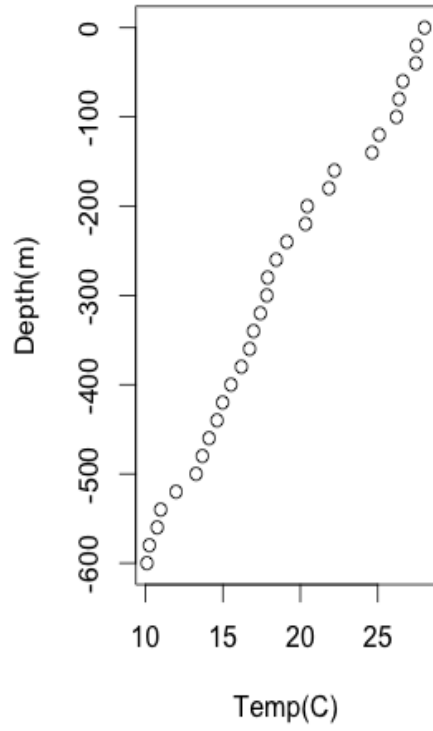
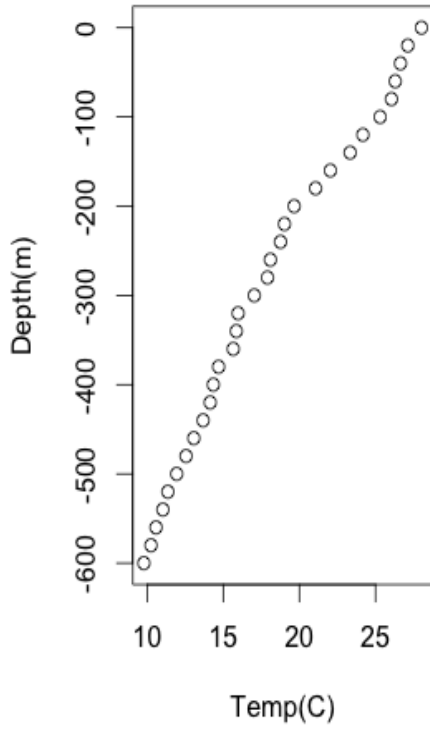
f) Madeira, Portugal, 2013.

Figures 6. Root mean square error (RMSE) comparisons plotted over time for three track derivation models from electronic tag data. RMSE is calculated by comparing each latitude and longitude estimate produced by the introduced hydrographic PCA model and two different light based models. Light data from Microwave Telemetry, Inc. model PTT-100s were run through the light-based model *TrackIt* to produce geolocation estimates (Figures a-c). Wildlife Computers, Inc. model PATs generate raw global positioning estimates that were put into a state-space model that incorporates satellite sea-surface temperature (SST) to derive the most accurate light-based locations (Figures d-f).

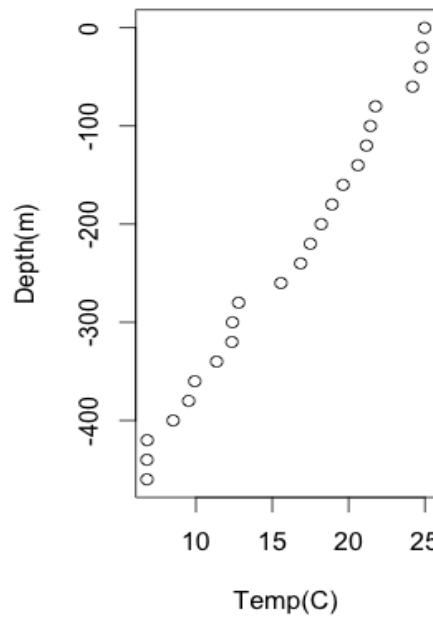
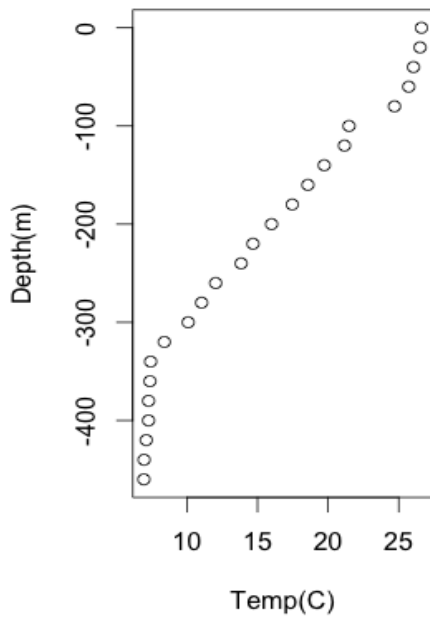
Figure 7.



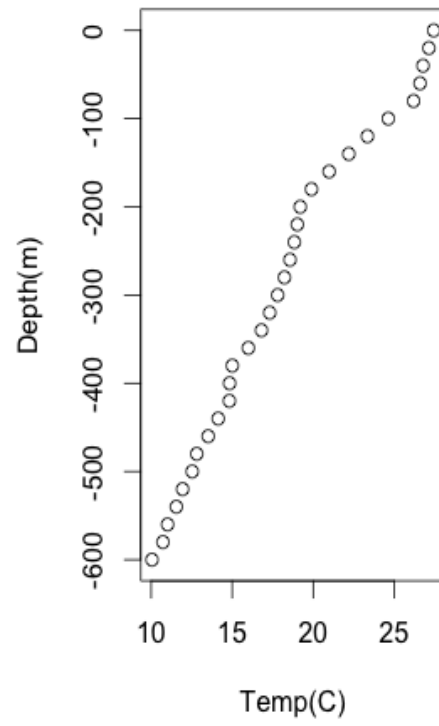
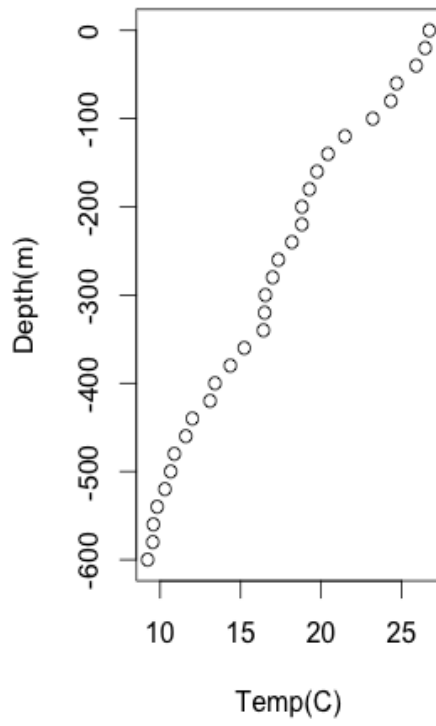
Figures 7. Root mean square (RMSE) plotted according to the length of tag deployment. Days-at-large (DAL) ranged from 9 to 120 days. A correlation can be seen in the longer tag deployments yielding larger error calculations



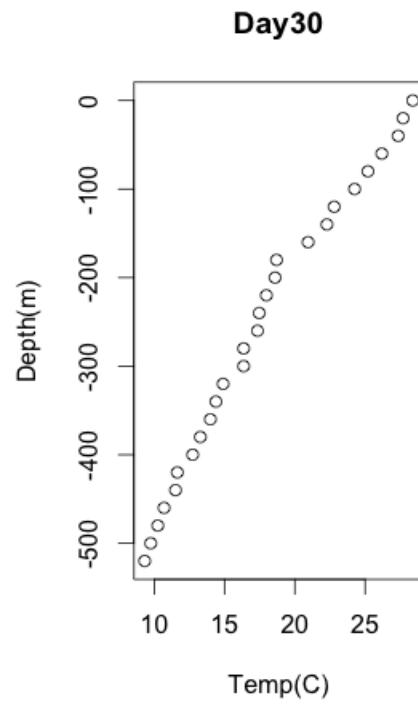
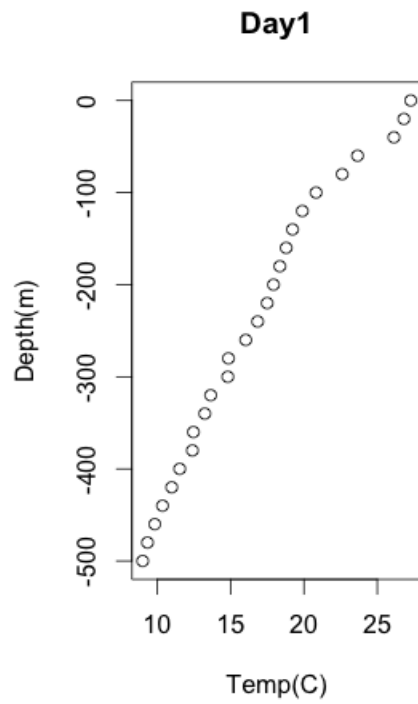
a) *Swordfish #61665*



b) *Swordfish #61699*

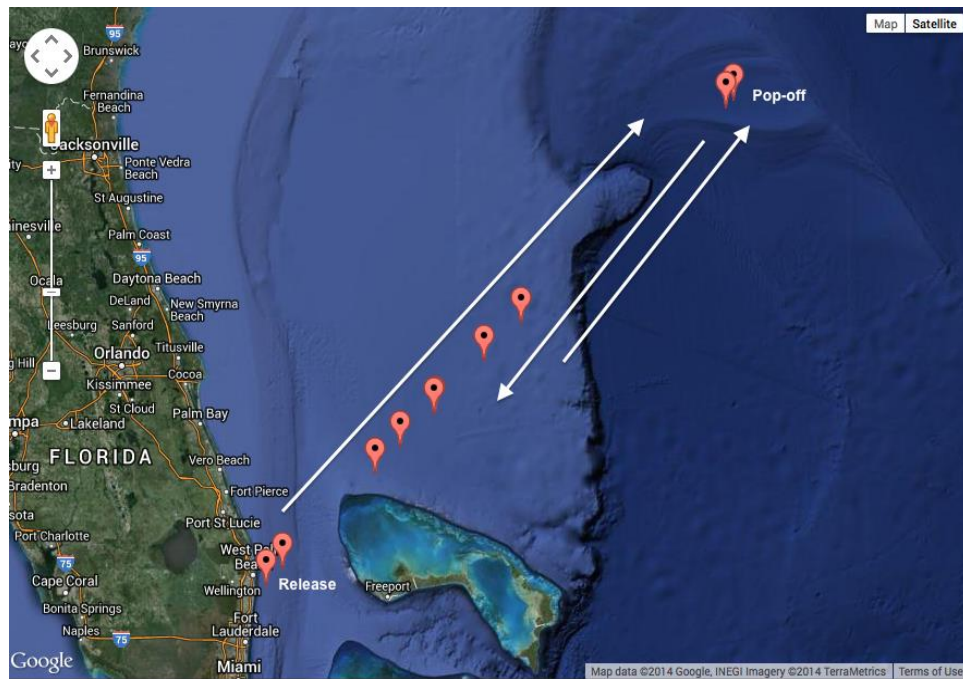
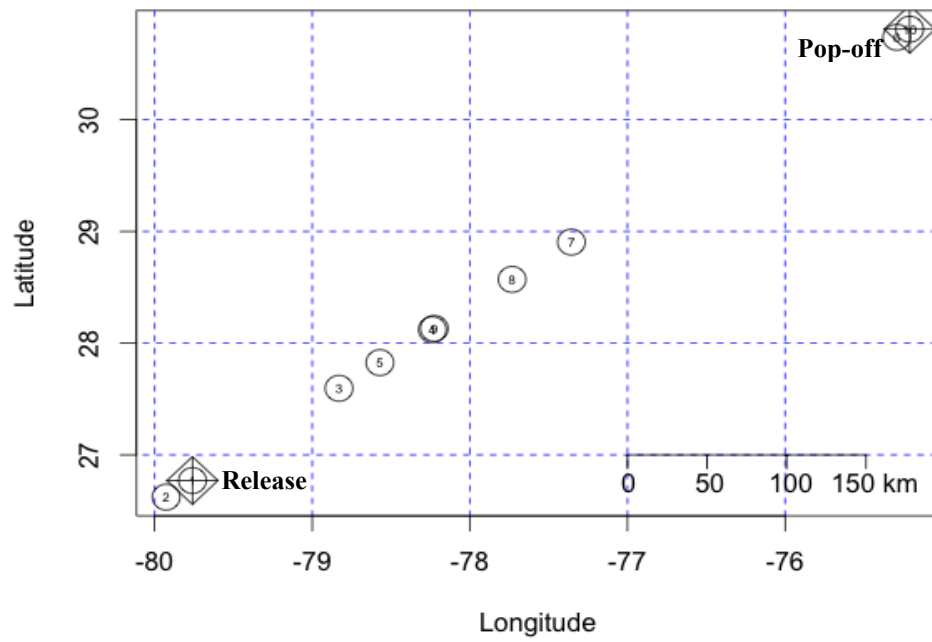


c) *Swordfish #86995*

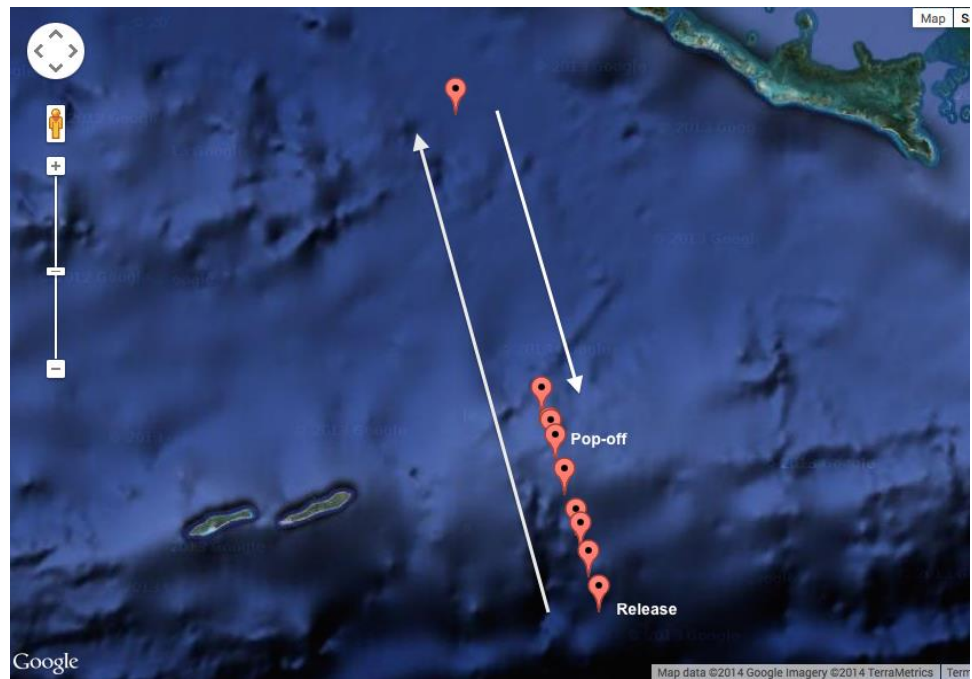
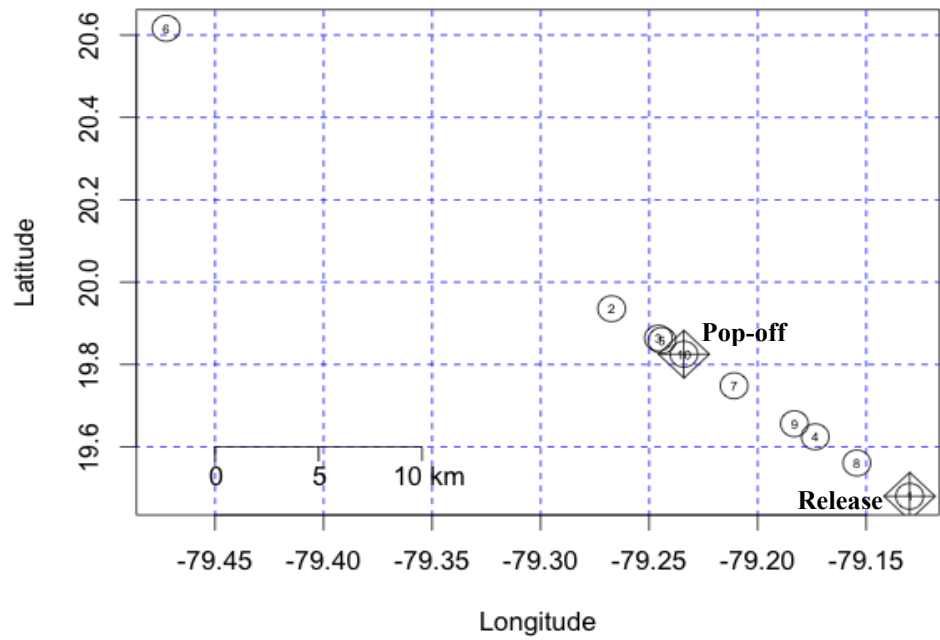


d) *Swordfish #88095*

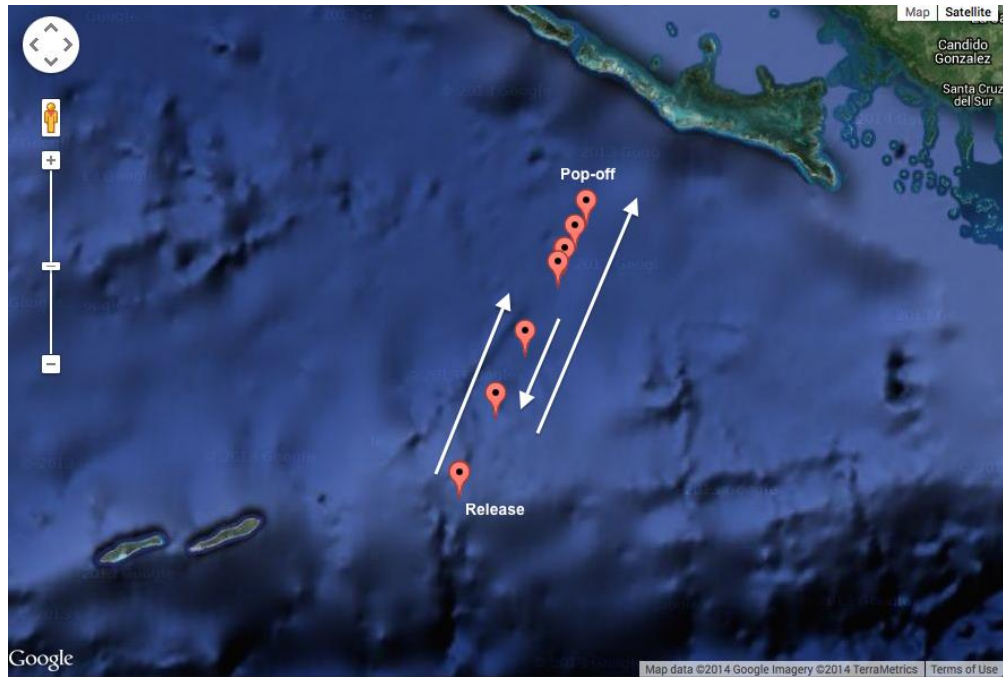
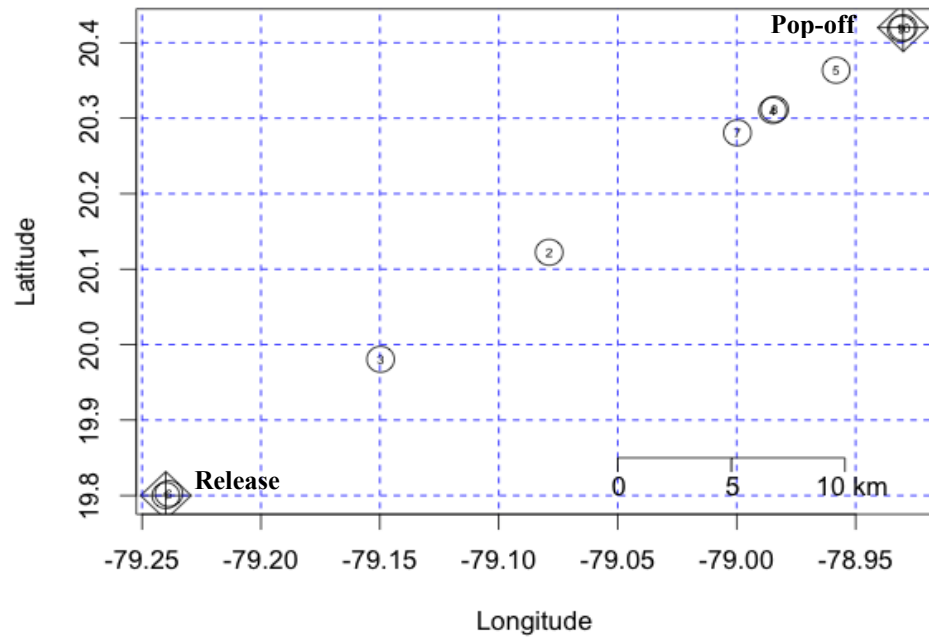
Figures 8. Temperature profiles recreated for the initial (left) and final (right) coordinates of swordfish tagged with Microwave Telemetry, Inc. PTT-100 tags (n=4). The temperature and depth data was interpolated and averaged at every 20 m depth each day.



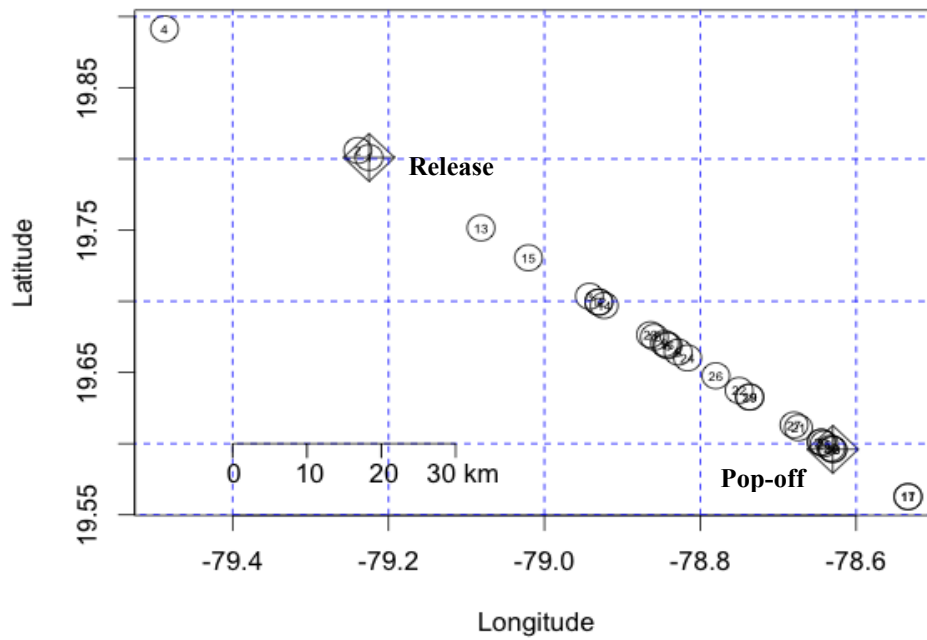
a) Swordfish #61699



b) Swordfish #61665



c) Swordfish #86995



d) Swordfish #88095

Figures 9. Fish tracks of swordfish tagged with Microwave Telemetry, Inc. model PTT-100 tags (n=4) created from the hydrographic PCA model. The locations of fish release and final tag pop off are highlighted. The top image is a latitude and longitude plot with each estimate labeled numerically by day. The bottom image is a Google Earth map of the general track and the directions taken by the fish according to our analysis.

Table 3. Average error (RMSE values) as given from two tag models (MT = Microwave Telemetry, Inc., WC = Wildlife Computers, Inc.). Average RMSE values and standard deviation (SD) are in kilometers.

	MT (<i>TrackIt</i>)	WC (<i>SST</i>)	Overall
Error	70.7	254.8	174.3
SD	61.9	83.3	118.9

Method Refinement

The focus of PCA is deriving few principal components from numerous variables. Therefore a primary objective is determining the number of PCs to use versus ignore. To support the use of the first as oppose to the first two or three PCs, a supplementary analysis was performed using seven PTT-100 datasets incorporating both the first and second PC. The algorithm to derive the spatial functions was adjusted as follows.

$$\begin{aligned} X_i &= aPC_{i,1} + bPC_{i,2} \\ Y_i &= cPC_{i,1} + dPC_{i,2} \end{aligned}$$

so that,

$$\begin{bmatrix} a \\ b \end{bmatrix} = \begin{bmatrix} PC_{1,1} & PC_{1,2} \\ PC_{n,1} & PC_{n,2} \end{bmatrix}^{-1} \begin{bmatrix} X_1 \\ X_n \end{bmatrix}$$

$$\begin{bmatrix} c \\ d \end{bmatrix} = \begin{bmatrix} PC_{1,1} & PC_{1,2} \\ PC_{n,1} & PC_{n,2} \end{bmatrix}^{-1} \begin{bmatrix} Y_1 \\ Y_n \end{bmatrix}$$

The results showed the use of both PCs reduced error only 43 percent of the time (Table 4). The total variance described by the first PC ranged from 87 to 94 percent with the second PC explaining two to twelve percent of total variance (Table 4). This is typical of PCA results that often find large variances associated with the first PC and then an abrupt drop-off. The primary goal is to reveal hidden simplified patterns in high dimensional data. The significance of our analysis can be lost if less important PCs are retained and used to derive our spatial functions.

For these trial PTT datasets ($n=7$), residual estimations or residual variance were calculated from the following equation, where Q is the principal component (PC), longitude (X), and latitude (Y) for each day i .

$$Q_i = \left(\frac{Q_1 + Q_n}{2} \right)$$

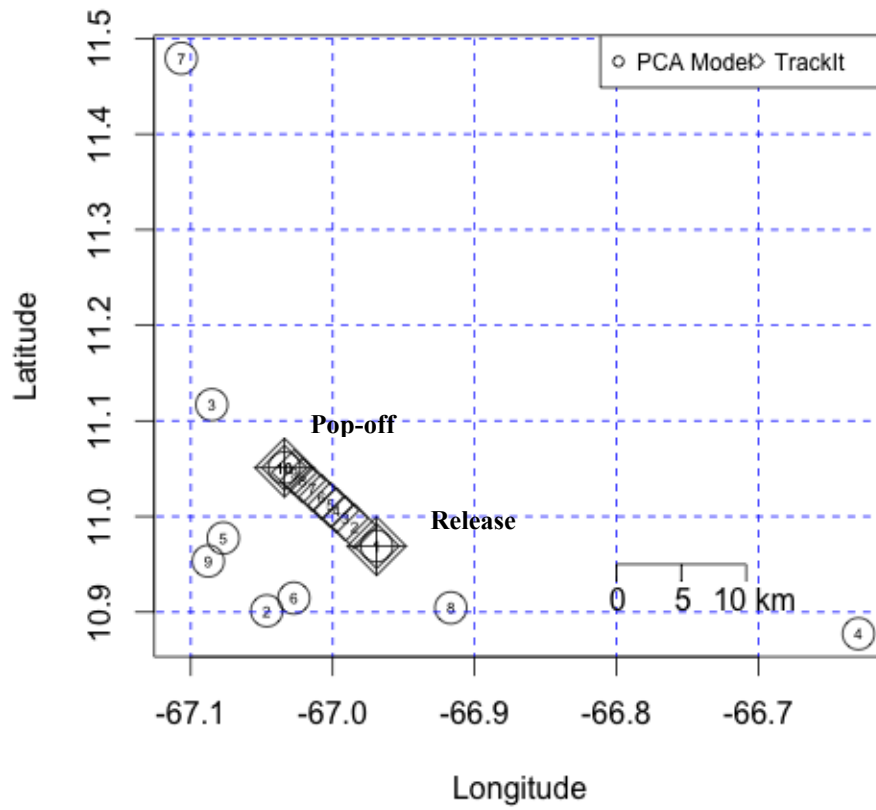
These estimations incorporated unobserved statistical error and transformed our initial linear trajectory, allowing nonlinear movements to be presented in our refined fish tracks

(Figures 10). The residual estimations showed a reduced average error (RMSE) in 57% of the trial PTT data used. However, overall average error calculated from the residual

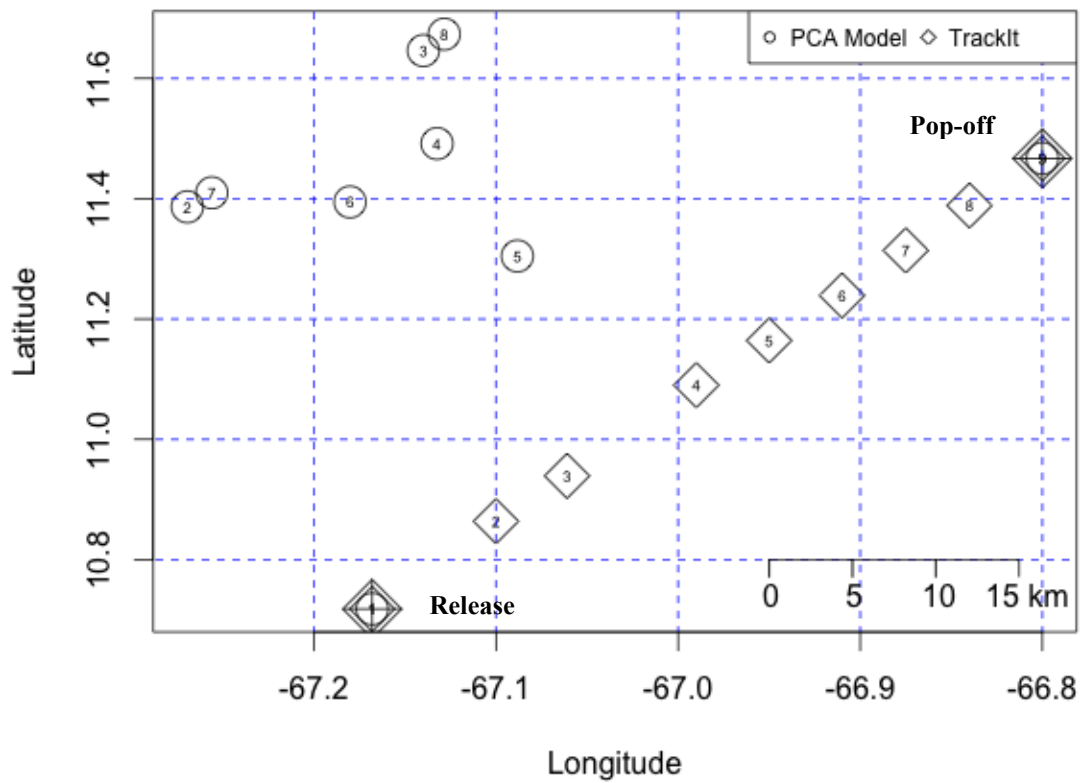
Table 4. Species code, tag ID number, average error (RMSE values) given by our PCA model analysis of PTT-100 (Microwave Telemetry, Inc.) data (n=7) incorporating the first computed principal component (PC) only, both the first and second PC, and the first PC residual calculations. Average RMSE values are in kilometers. The variances described by the respective PCs are given as a percentage.

Species Code	Tag ID	1 PC RMSE	2 PC RMSE	1 PC Residual RMSE	PC1 Var. (%)	PC2 Var. (%)
BUM	24523	15.3	2.6	17.5	91	7.5
BUM	84351	55.5	95.4	44.3	87	9
BUM	34233	40.8	34.5	36.6	90	9
BUM	41333	75.9	83.1	62.5	88	10
BUM	59080	27.7	42.7	153.1	94	5.2
BUM	35687	156.5	183.9	178.7	90	6.6
BUM	84363	192.8	181.3	157	89	10

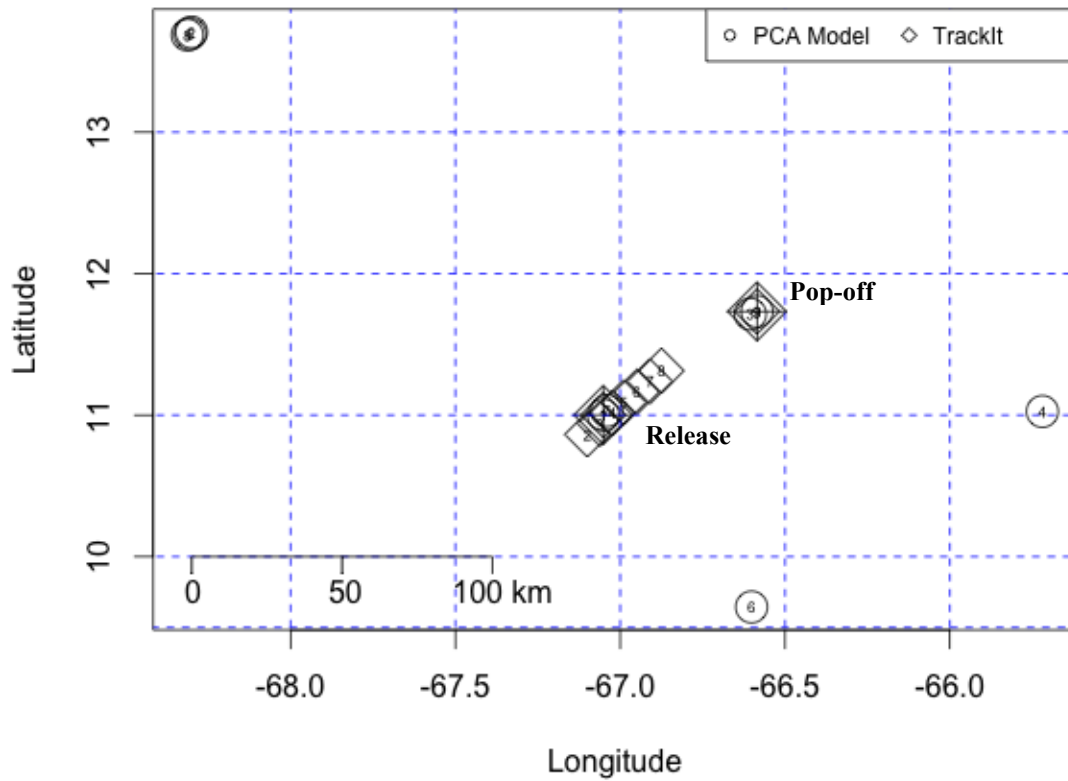
Figures 10.



a) BUM 24523; Caracas, VZ, May 15, 2008 – May 25, 2008



b) BUM 34233; Caracas, VZ, May 17, 2008 – May 27, 2008



c) BUM 59080; Caracas, VZ, April 18, 2009 – April 27, 2009

Figures 10. Estimates of marlin (n=3) tagged with Microwave Telemetry Inc. PTT-100 tags (n=3) as given by the PCA model analysis and residual calculations.

estimations was the largest at 92.8 km. This is approximately three kilometers more than the error estimated from using of the first two PCs (89.9 km) and over ten kilometers more than the trials using the first PC only (80.6 km). These results support our original use of the 1st PC only as the most efficient method for representing this spatial data in order to estimate fish movement. Nevertheless, preliminary assessments such as this should be conducted for future analyses on additional tag data. The reduced error in three of the seven trials incorporating both PCs demonstrates the potential for more than one PC to capture the most variance among the original data and subsequently provide more accurate location estimates.

DISCUSSION

The PCA model described represents a completely new approach to tracking methodology using electronic archival tag data. Since the development of light-based methods to generate global positioning of tagged individuals, many studies have aimed at improving the precision of these methods, but none deviated from them with a new technique. Furthermore, no study has attempted to use archived temperature and depth data alone to estimate the geographical locations of tagged marine organisms.

The comparison analyses showed on average this methodology works within 174.3 km of the light-based geolocation estimates. Multiple studies have demonstrated that light-based geolocation can work well within this error margin (Ekstrom 2004, Hill and Braun 2001, Lam et al. 2010, Musyl et al. 2003, Nielsen et al. 2006, Nielsen and Sibert 2007, Shaffer et al. 2005, Sibert et al. 2003, Teo et al. 2004). Nielsen and Sibert (2007) showed that the most probable tracks are reconstructed within 0.5-1 degree longitude and 1-2 degrees latitude of the true value. However, these studies have all been performed using tags deployed on near-surface fish or with simulated data. Furthermore, these studies show light-based estimations up to 4 degrees latitude off the actual position when in temporal proximity to the equinox (Schaefer & Fuller 2006, Lam et al. 2010). Previous attempts to track swordfish demonstrate how current archival tags, light-processing algorithms, and resulting geographical positioning are not suitable for fine scale movement (Musyl et al. 2001).

This study utilizes the diel movements of the tagged fish to record and recreate hydrographic properties of the water column. In what can essentially be called “hydrographic-based geolocation,” this analysis takes advantage of satellite data that can reveal the qualitative patterns of our oceans circulation. Similar to tracking storms and weather patterns, this study demonstrates how PCA of localized oceanographic conditions can be used to estimate the movement of marine animals.

The analysis makes use of distinct differences in the temperature profile structures to assess how far the fish has moved horizontally. Therefore the model will work best when tags are exposed to frontal zones where hydrographic properties vary dramatically over a relatively short distance. This allows the temperature profiles to exhibit a stronger

signal for the PCA to attribute to distinct locations. Frontal regions include along shelf breaks or within seismic activity where thermal intrusions take place. Studies show a strong relationship between fronts and fish abundance (Podesta et al. 1993). Our results show a correlation between the error calculations and length of tag deployment (Figure 7). This is to be expected as the longer days at large (DAL) are subject to changing temperature variability of water masses.

Swordfish provide us with valuable data due to their large diel vertical movements. As the tagged swordfish makes their vertical migration, real time records of temperature and pressure describe an extensive temperature profile of that water column. Temperature and depth recordings by a tag are functions of local hydrography and movement activity. Our model incorporates environmental values much like those commonly used in SST-incorporating models. The use of these values allows us to take advantage of the ability of archival tags to record ambient variables with precision. Much like the SST models, we are able to link the geographical positions with the physical environment described by the tag data (Shaffer et al.2005). With our model, however we are able to utilize the entire water column rather than the first few meters. This information is particularly useful when describing individual behavior, and habitat preferences. Much like SST, these observations are most effective when the temperature signal in a region is spatially stratified (Lam et al. 2011). However, when using data from swordfish deployments, our temperature utilization of the entire water column moderates this as a restricting factor. Due to the natural properties of the water column, temperature has a stronger signal at depth.

The data used for the PCA input greatly influence the model outcome. In particular, the profiles created for day 1 and day n , must have detailed and complete profiles in order for the model work effectively. These two temperature profiles determine how all other profiles are evaluated in terms of the variance they represent. The analysis uses the variation between these two profiles to determine appropriate movement based on the variability all other profiles exhibit. For instance if these profiles are incomplete or erratic, the PCA will expect all profiles to be similarly structured. Thus, any “normal” reconstructed profile would be assigned a dramatically different PC

value. This would result in inaccurate latitude and longitude calculations that would place the fish farther away than most likely positioned

The two tag models used for this study provided an opportunity to assess what data works best with our model. The tag models and respective light-based geolocation estimates yielded a difference of 184 km in average RMSE values (Table 3). The PTT-100 HR tags provide the raw temperature and pressure (converted to depth) data at frequent intervals necessary to construct a precise vertical temperature profile (Figures 1 and 7). However, the low-resolution light data does not allow light-based models to work to their best ability. The PAT light data and IGFA/Stanford light-based model provided statistically robust geolocation estimates. The histogram bin data comprised of eight temperature and depth measurements did not allow the PCA to capture the full thermal stratification of each day. Limited memory storage of the tags mean longer deployments require prolonged sampling intervals. Depending on the number of days at-large, this can lead to multiple days of missing or insufficient PDT data that doesn't allow us to create a vertical temperature profile. In those cases where profiles could not be reconstructed due to lack of data, coordinate estimates were not made for the respective days. Thus, tracks created for analysis purposes were in some cases with marlin shorter than the actual tagged days at-large (Table 1).

Although, research has provided short-term movements and general behavior patterns, little is known regarding their movement in-between the established foraging and spawning grounds. The lack of tagging studies in the past stems from individual tag costs, and inefficient use of data retained. This includes incoherent light-based geolocation estimates generated from the minimal light records transmitted. Our hydrographic model will give estimates of swordfish locations each day, allowing us to create a general track of day-to-day movement. This will assist in defining activity patterns not yet established for swordfish, and provide stock assessments with much needed knowledge regarding swordfish stock structure.

This study supports the use of this model as an ideal global positioning estimator that should be explored further. Double-tagging studies using both satellite telemetry tags and archival tags should be considered for future assessments of this model. The ample data provided by archival tags coupled with the geographical precision of acoustic

tags will allow direct comparison between our model estimates and actual locations. An increased effort in sharing tag data preferably from double-tagged animals will provide a more objective way of determining the accuracy of this model. In addition to the gathering of more tag data, this model should be expanded to incorporate auxiliary environment information. Similar to the way in which SST has been used to refine light-based geolocation estimates, satellite temperature and depth data can benefit our model. Hydrographic data can be accessed from Expendable Bathythermographs (XBTs) deployed throughout most oceanic regions. A PCA performed on temperature profiles from a high-resolution data-assimilative ocean circulation model would give EOF modes that better describe the pattern of thermal variability among the water masses sampled. The incorporation of this data into the analysis of tag data would generate estimations, in theory, closer to actual fish locations.

In conclusion, a PCA-based model incorporating local hydrographic data is a compatible method for generating estimates of satellite tagged fish. Despite the limitations of tag data accessible, this study provided encouraging results. Unlike “best fit” tracks created from light-based models, the PCA model assumes linearity, so tracks generated by this model will be based on linear vectors (Figures 2a-f). However, these estimates are calculated at frequent enough intervals (e.g., every day) that swordfish movement can be recreated more precisely than prior methods. Furthermore, the PCA method utilizes data that are not distorted by weather conditions or time of year, thus are more consistently accurate. A model of this caliber will provide useful information on fine-scale movement of swordfish. Our new approach to improve tracking methods of this species adds to a wide range of geolocation methodologies (Lam et al 2008). This allows researchers to choose the model that will work best for their study.

Tagging studies and geolocation estimation procedures have significant resource management applications. Taking into consideration the lack of knowledge of the Atlantic stock structure and population boundaries, the continued use of electronic tags is highly encouraged. The use of PSATs in combination with global positioning estimation models provides valuable information regarding the complex behavior of swordfish (Abascal et al 2015). The information provided helps describe the dynamics of this species and reduce those uncertainties prevalent in swordfish stock assessments.

LITERATURE CITED

- Abascal, F.J., Mejuto J., Quintans M., Garcia-Corets B., Ramos-Cartelle, A. 2015. Tracking of the broadbill swordfish, *Xiphias gladius*, in the central and eastern North Atlantic. *Fisheries Research*. 162: 20-28.
- Arnold, G., Dewar, H. 2001. Electronic tags in marine fisheries research: a 30-year perspective. In: *Electronic tagging and tracking in marine fisheries*, edited by Sibert J.R., Nielsen JL Kluwer Academic Publishers, Dordrecht, The Netherlands, -64.
- Arocha, F., Moreno, C., Beerkircher, L., Lee, D.W., Marcano, L. 2003. Update on growth estimates on swordfish, *Xiphias gladius*, in the northwestern Atlantic. *Col Vol Sci Pap ICCAT*. 55: 1416-1429.
- Carey, F.G., Robison, B.H. 1981. Daily patterns in the activities of swordfish, *Xiphias gladius*, observed by acoustic telemetry. *Fish Bulletin*. 79: 277-292.
- Dewar, H., Prince E.D., Musyl, M.K., Brill, R.W., Sepulveda, C., Luo, J., Foley, D., Orbesen, E.S., Domeier, M.L., Nasby-Lucas, N., Snodgrass, D., Laurs, R.M., Hoolihan, J.P., Block, B.A., McNaughton, L.M. 2011. Movements and behaviors of swordfish in the Atlantic and Pacific Oceans examined using pop-up satellite archival tags. *Fisheries Oceanography*. 20: 3, 219-241.
- Ekstrom, P.A. 2004. An advance in geolocation by light. *Mem. Nat'l Inst. Polar Res., Spec*. 58: 210-226.
- Evans, K., Baer, H., Bryant, E., Holland, M., Rupley, T., Wilcox, C. 2011. Resolving estimation of movement in a vertically migrating pelagic fish: Does GPS provide a solution? *Journal of Experimental Marine Biology and Ecology*. 398: 9-17.
- Faugeras, B., Maury, O. 2007. Population movements: From an individual-based

representation to an advection-diffusion equation. *Journal of Theoretical Biology*. 247: 837-848.

Fenton, J. "Post-Release survival and habitat utilization of juvenile swordfish in the Florida Straits." Masters thesis, Nova Southeastern University Oceanographic Center (2010).

Govoni, J. J., Laban, E.H., Hare, J.A. 2003. The early life history of swordfish (*Xiphias gladius*) in the western North Atlantic. *Fish Bulletin*. 101:778-789.

Graves J.E., Horodysky A.Z. 2010. Asymmetric conservation benefits of circle hooks in multispecies billfish recreational fisheries: a synthesis of hook performance and analysis of blue marlin (*Makaira nigricans*) postrelease survival. *Fishery Bulletin*. 108(4): 433-441.

Heemsoth A. 2010. Diet composition of swordfish, *Xiphias gladius*, within the Straits of Florida. Nova Southeastern University, p79.

Hill R.D., Braun M.J. 2001. "Geolocation by light level – the next step: latitude." In *Electronic Tagging and Tracking in Marine Fisheries*, edited by J.R. Sibert & J. Nielsen. 315-330. Kluwer Academic Publishers.

ICCAT, Standing Committee on Research and Statistics. "Report of the 2009 Atlantic Swordfish Stock Assessment Session." 2009. Madrid, Spain.

International Game Fish Association. "International Great Marlin Race." 2013. <http://igmr.igfa.org/Conserve/IGRM.aspx>.

Jonsen, I.D., Myers, R.A., Flemming, J.M. 2003. Meta-analysis of animal movement using state-space models. *Ecology*. 84(11): 3055-3063.

Lam, C.H., Nielsen, A., Sibert, J.R. 2008. Improving light and temperature based

geolocation by unscented Kalman filtering. *Fisheries Research*. 91: 15-25.

Lam, C.H., Nielsen, A., Sibert, J.R. 2010. Incorporating sea-surface temperature to the light based geolocation model TrackIt. *Marine Ecology Progress Series*. 419: 71-84.

Lam, C.H., Tsonotos, V.M. 2011. Integrated Management and Visualization of Electronic Tag Data with Tagbase. *PLoS ONE* 6(7): e21810. doi:10.1371/journal.pone.0021810.

Lerner, J.D., Kerstetter D.W., Prince, E.D., Mariano, A., Orbesen, E., Snodgrass, D., McManus, L., Thomas, G.L. 2013. Swordfish (*Xiphias gladius*) vertical distribution and habitat use in relation to diel and lunar cycles in the western North Atlantic. *Transactions of the American Fisheries Society*. 142: 95-104.

Levesque, J.C., Kerstetter, D.W. 2007. First observations on the re-established southeast Florida recreational swordfish tournament fishery. *Florida Scientist*. 70: 284-296.

Lisovski, S., Hewson, C.M., Klaassen, R.H.G., Korner-Nievergelt, F., Kristensen, M.W., Hahn, S. 2012. Geolocation by light: accuracy and precision affected by environmental factors. *Methods in Ecology and Evolution*. 3: 503-612.

Loefer, J.K., Sedberry, G.R., McGovern, J.C. 2007. Nocturnal depth distribution of western North Atlantic swordfish (*Xiphias gladius*, Linnaeus, 1758) in relation to lunar illumination. *Gulf and Caribbean Research*. 19(2): 83-88.

Luckhurst, B.E. 2007. Large pelagic fishes in the wider Caribbean and north-west Atlantic Ocean: movement patterns determined from conventional and electronic tagging. *Gulf and Caribbean Research*, 19(2): 5-14.

Mariano, A.J., Hitchcock, G.L., Ashjian, C.J., Olson, D.B., Rossby, T., Ryan, E., Smith,

- S.L. 1996. Principal component analysis of biological and physical variability in a Gulf Stream meander crest. *Deep-Sea Research I*. 43(9): 1531-1565.
- Microwave Telemetry I. 2013. Microwave Telemetry, Inc, Columbia, MD.
- Musyl, M.K., Brill, R.W., Boggs, C.H., Curran, D.S., Kazama, T.K., Seki, M.P. 2003. Vertical movements of bigeye tuna (*Thunnus obesus*) associated with islands, buoys, and seamounts near the main Hawaiian Islands from archival tagging data. *Fisheries Oceanography*. 12(3):152-169.
- Nakamura, I. 1985. Billfishes of the world. *FAO Fish Synop*. 125: 58p.
- Nielsen, A., Sibert, J.R. 2007. State-space model for light-based tracking of marine animals. *Canadian Journal of Fisheries and Aquatic Sciences*. 64: 1055-1068.
- Nielsen, A., Bigelow, K.A., Musyl, M.K., Sibert, J.R. 2006. Deriving light-based geolocation by including sea surface temperature. *Fisheries Oceanography*. 15(4): 314-325.
- Neilson, J.D., Smith, S. 2010. Update on the Canadian program for pop-up satellite archival tagging of swordfish. *Collect. Vol. Scientific Papers. ICCAT*, 65(1): 229-240.
- Podesta G.P., Browder, J.A., Hoey, J.J. 1993. Exploring the association between swordfish catch rates and thermal fronts on United-States longline grounds in the Western North-Atlantic. *Cont Shelf Res*. 13(2-3): 253-27.
- Schaefer, K., Fuller, D. 2002. Movements, behavior, and habitat selection of bigeye tuna (*Thunnus obesus*) in the eastern equatorial Pacific, ascertained through archival tags. *Fish Bulletin*. 100: 765-788.

- Shaffer, S.A., Tremblay, Y., Awkerman, J.A., Henry, R.W., Teo, S.L.H., Anderson, D.J., Croll, D.A., Block, B.A., Costa, D.P. 2005. Comparison of light- and SST-based geolocation with satellite telemetry in free-ranging albatrosses. *Marine Biology*. 147: 833-843.
- Sedberry, G.R., Loefer, J.K. 2001. Satellite telemetry tracking of swordfish, *Xiphias gladius*, off the eastern United States. *Marine Biology*. 139: 355-360.
- Sepulveda, C.A., Knight, A., Nasby-Lucas, N., Domeier, M.L. 2010. Fine-scale movements of the swordfish *Xiphias gladius* in Southern California Bight. *Fisheries Oceanography*. 19(4): 279-289.
- Sibert, J.R., Musyl, M.K., Brill, R.W. 2003. Horizontal movements of bigeye tuna (*Thunnus obesus*) near Hawaii determined by Kalman filter analysis of archival tagging data. *Fisheries Oceanography*. 12(3): 141-151.
- Taylor, R.G., Murphy, M.D. 1992. Reproductive biology of the swordfish *Xiphias gladius* in the Straits of Florida and adjacent waters. *Fish Bulletin*. 90: 809-816.
- Teo, S.L.H., Boustany, A., Blackwell, S., Walli, A., Weng, K.C., Block, B.A. 2004. Validation of geolocation estimates based on light level and sea surface temperature from electronic tags. *Mar Ecol Prog Ser*. 283: 81-98.
- U.S. Department of Commerce, National Oceanic and Atmospheric Administration, National Marine Fisheries Service. Office of Sustainable Fisheries. Highly Migratory Species Management Division. *Final Fishery Management Plan For Atlantic Tuna, Swordfish, and Sharks*. Silver Spring, MD. 1999.
- U.S. Department of Commerce, National Oceanic and Atmospheric Administration. National Marine Fisheries Service, Office of Sustainable Fisheries, Highly Migratory Species Management Division. *Final Consolidated Atlantic Highly Migratory Species Fishery Management Plan*. Silver Spring, MD. 2006.

U.S. Department of Commerce, National Oceanic and Atmospheric Administration.
National Marine Fisheries Service, Office of Sustainable Fisheries, Highly
Migratory Species Management Division. *Final Amendment 3 to the Consolidated
Atlantic Highly Migratory Species Fishery Management Plan*. Silver Spring, MD.
2010.

U.S. Department of Commerce, National Oceanic and Atmospheric Administration,
National Marine Fisheries Service. *Synopsis of the biology of the swordfish,
Xiphias gladius Linnaeus*, by Palko, B.J., Beardsley, G.L., Richards, W.J. Tech
Rep. NMFS Circ. 1981.

Wildlife Computers I. 2014. Wildlife Computers, Inc, Redmond, WA.

Wilson, S.G., Lutcavage, M.E., Brill, R.W., Genovese, M.P., Cooper, A.B., Everly, A.W.
2005. Movements of bluefin tuna (*Thunnus thynnus*) in the northwestern Pacific
Ocean recorded by pop-up satellite archival tags. *Marine Biology*. 146: 409-423.

